Failure Mechanisms of Balanced Armature Receivers under Drop and Shock Loading Conditions

MSc Thesis

Bas Haayen

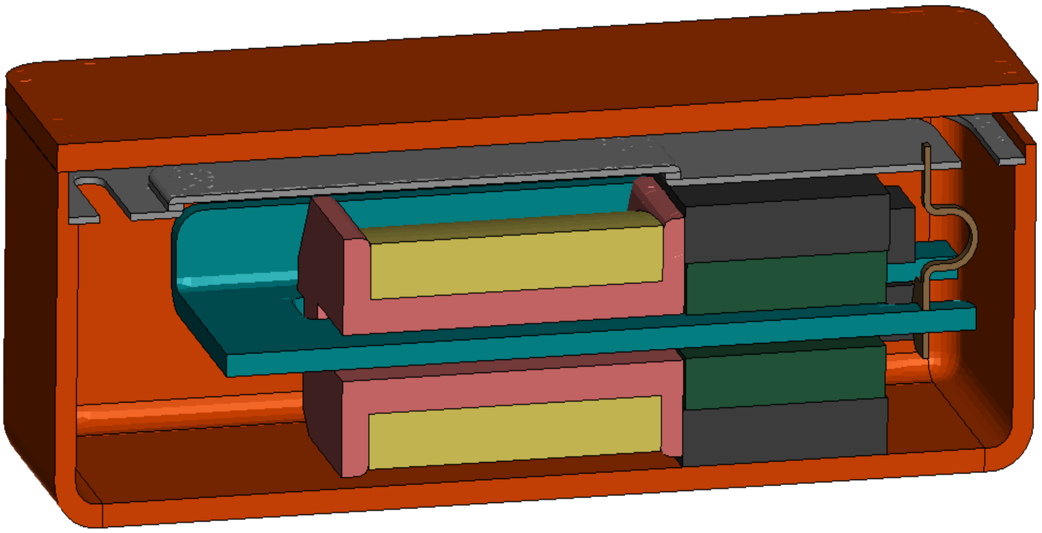

Failure Mechanisms of Balanced Armature Receivers under Drop and Shock Loading Conditions

by

Bas Haayen

in partial fulfillment of the requirements for the degree of

Master of Science
in Biomedical Engineering

at the Delft University of Technology,
to be defended publicly on Friday September 15, 2023 at 10:00 AM.

Student number:	4422929	
Project duration:	January, 2023 – September, 2023	
Thesis committee:	Prof. Dr. P. J. French,	TU Delft
	Dr. ir J. F. L. Goosen,	TU Delft
	M. Colloca, PhD.	Sonion Nederland B.V.

This thesis is confidential and cannot be made public until September 16, 2024.

An electronic version of this thesis is available at `http://repository.tudelft.nl/`.

TU Delft

Abstract

Balanced armature receivers are electroacoustic transducers that are mostly integrated in hearing aid devices or pro audio products. The balanced armature receiver is a key component for the performance of hearing aids as it converts the processed electrical signal into sound waves. Failure or defects of the balanced armature receiver are problematic for the end user. The balanced armature receivers are tested under shock loading conditions. But in order to really understand the failure mechanisms that arise, it is important to gain insight in the mechanical response of the structure. A combination of Finite Element Analysis, experiments and measurements will help understanding the failure mechanisms in more depth. Better understanding will lead to the possibilities to create more robustness which is a value for the end used.

First, it is important to understand how mechanical shock loads affect the balanced armature receiver. The performance is defined and measured as sound pressure output and Total Harmonic Distortion (THD) before and after shocking the receiver at different acceleration levels. To properly study the impact analysis of the balanced armature receiver it is essential to have a controlled shock environment with consistent repeatability. The controlled environment allows also for building virtual prototyping. A half sine pulse is derived from the measurement results of the impact test set-up. The explicit finite element software from Ansys LS-Dyna is used to model the shock wave during impact as a function of time. The balanced armature receiver geometry CAD drawing must be prepared properly to be suitable for FE modelling. The FE model is built with all the corresponding pre-processing steps. In parallel different experiments and measurements are performed to gain confidence in the FE models. One of the major challenges in measuring impact responses in this study is the size and the closed casing of the balanced armature receiver. It is possible to test difference components separately. One of the most important parts, the armature, is tested separately for its eigenfrequencies and mode shapes. The deformation of the membrane is measured before and after shock via an optical profiler.

The results of the finite element models indicate that two components, the armature and membrane, are the most prone to damage. In the hinges of the membrane high stress concentrations can be found. To highlight the critical regions, an input acceleration of 19000 [g] is applied in the finite element model. The von Mises stress in the hinges of the membrane exceed the yield criteria, which leads to plastic strain and permanent deformation. The plastic deformation corresponds with the off-set found during the measurements of approximately 25 μm in depth. The armature experience high stresses beyond the yield criteria in the hinge region and around the drive pin. The results of these plastic deformations lead to an increase in the total harmonic distortion.

The virtual prototype of the membrane with a 100 μm, instead of 50μm, thickness to increase the stiffness resulted in a more robust response under drop and shock loading conditions. The internal energy, which is defined by the energy stored due to deformation, has decreased, as well as the amount of plastic strain in the hinges. The improved robustness does come at the cost of a decrease in the sound pressure output. Adding shock plates between the permanent magnets and the armature resulted in a decrease of internal energy. The maximum contact force between the armature against the magnets went down with almost 20%. The implementation of finite element modelling in understanding the failure mechanisms of balanced armature receivers under drop and shock loading conditions and the use for virtual prototyping has been proven to be insightful and promising for future work.

Acknowledgements

This thesis marks the end of my study period at the TU Delft. I am grateful to have had the opportunity to work in this exciting field with the latest technological developments and innovations in the healthcare industry. However during this journey of obtaining a bachelor in mechanical engineering and a master in biomedical engineering there were many people that helped and supported me to accomplish this.

First of all, I would like to express my sincere gratitude to my TU Delft supervisor Paddy French who was there to guide and help me from the beginning of my internship all the way to the end of the thesis. The thesis could not have been done without my other supervisor from Sonion Nederland B.V, Michele Colloca, who gave me the opportunity to carry out my thesis at Sonion Nederland B.V. and guided me along the way. Furthermore I would like to thank Oleg Antoniuk and Thibault Gauran from the modelling and simulation department for sharing their knowledge and advise. Another final thanks to the people in Sonion Nederland B.V. who shared their knowledge and helped me with different experiments of the thesis.

Finally, I would like to thank my parents and my brother for always giving the complete support and confidence. Also I would like to give special thanks to my girlfriend whom I could always counts on. Whether it was providing me with feedback or just being there for the good times. Both helped me to carry on and finish this adventure.

Bas Haayen
Delft, September 2023

Contents

List of Abbreviations

3D	Three Dimensional
BTE	Behind The Ear
BNC	Bayonet Neil Concelman
CAD	Computer Aided Engineering
CFL	Courant-Friedrichs-Lewy
dB	Decibel
DSP	Digital Signal Processor
DSS	Development Support Services
EPS	Effective Plastic Strain
FEA	Finite Element Analysis
FEM	Finite Element Method
FRF	Frequency Response Function
ITE	In The Ear
JEDEC	Joint Electron Device Engineering Council
ODE	Ordinary Differential Equation
PDE	Partial Differential Equation
RMS	Root Mean Square
R&D	Research and Development
SPL	Sound Pressure Level
THD	Total Harmonic Distortion

List of Figures

List of Tables

1 Introduction

1.1. Introduction

Hearing aids are devices used world wide in the hearing health that contributes to the well-being of millions of people. A report of the SiRM (Strategies in Regulated Markets) estimates that only in the Netherlands there are around 800.000 hearing aid users [1]. Since the first developments of ear trumpets the hearing health has made great developments. As technology advances, so does the hearing aid technology. Hearing aids have become an advanced piece of technology that has become a part of people their daily lives. A hearing aid during its lifetime is subjected to all different kind of shock environments. This includes the possibility of dropping the device, transport and other accidents that potentially damage the hearing aids and their components. Damage can result in reduced performance quality, distorted output or permanent failure.

In general a hearing aid consist of at least the following components: a microphone, an amplifier, a battery, user controls and a receiver [2]. A receiver refers in this investigation to a balanced armature receiver. Balanced armature receivers are electroacoustic transducers that are integrated in hearing aids or pro-audio devices. The balanced armature receiver converts an electrical signal into a sound output. The majority of the type of receivers in hearing aids are balanced armature receivers, occasionally referred to as driver or transducer. In the remainder of this report, the receivers will be unequivocally referred to as balanced armature receivers or receivers for short.

The name "balanced armature receiver" finds its origin in the way they are designed. An armature, a metal strip, is accurately balanced between magnets and is driven by a core-less coil. The balanced armature receiver, as a component of hearing aids, is exposed to multiple external factors that might cause the receiver to be damaged and produce a distorted signal or complete failure. One of these reasons is the exposure to mechanical shocks, such as dropping of the device. An improvement of robustness of the design is a desired wish from the engineer, the customer and the end user.

To better understand the structural response, failure mechanisms and possibilities for improvement, it is important to look into the different types of shock environments that can be controlled, model and analysed. One of the major difficulties is to understand what is happening during the shock impact inside the receiver. The receiver is a very small (see fig 1.1) closed structure with a casing and cover which makes it very challenging to make good observations. Hereby a finite element model will help to understand this process and thus finding the failure mechanisms. This gained knowledge and insight of finite element model together with the experiments and validation will help the design of more robust balanced armature receivers.

Currently, there is a wide range of balanced armature receivers with different geometries and specifications. In this study the focus will be on one specific product of a balanced armature receiver, that is the 3100 model provided by Sonion. If a methodology and documentation can be provided to find the failure mechanisms of this product under drop and shock loading, it could contribute to improving the design of balanced armature receivers.

1.2. Relevance

It is important that the engineers properly understand the shock response and why that leads to failure. Improvements can be made for a more robust design and thus a longer and more reliable lifetime of the product. From the perspective of the end user, there are hearing aids on the market that have the receiver in the auditory ear canal. This makes it even more important for the user that the product is reliable to use after it has been subjected to shock. Additionally, improving shock resistance has an economic incentive. The company has a market advantage if they can prove that their products can withstand a certain level of shock.

Furthermore in this study it will be relevant to explore the possibility to integrate the finite element modelling process into virtual prototyping. If the methodology can be laid out, future analysis could easily be implemented with this knowledge.

To the knowledge of the author proper research including modelling and 3D simulation together with experiments and validation in the lab on balanced armature receivers under drop and shock loading conditions has not, or to little extend, been conducted.

Figure 1.1: The 3100 Sonion balanced armature receiver

1.3. Aim of the Thesis

This Thesis aims to give a better understanding of the mechanical failure mechanisms of balanced armature receivers under drop and shock loading conditions with the help of Finite Element Analysis, a methodology and experimental data.

This includes the following:

- Creating a controlled shock environment, measurements and a methodology to implement and correlate this in the FE models.
- Preparation, pre-processing and building the FE models and simulations. Different simulations to study the effect of magnitude, duration and orientation on the response of the receiver. Methodology to check the quality of the finite element model including the different post processing techniques.
- Experiments must be performed to study the effects of the shock on the receiver, as well as experiments to build confidence and validation of the models. This will be done via modal analysis and final displacement configurations.
- Finally recommendations on how to manipulate and improve the mechanical response of a balanced armature receiver.

1.4. Outline of the thesis

- Chapter 2 "Background Information" contains an explanation on the working principle of the balanced armature receiver. The components are introduced and its function explained.
- Chapter 3 "Modelling and Simulation" discusses the necessary theoretical background, methodology for the modelling & simulation and provides methodology for multiple modelling experiments.
- Chapter 4 "Experimental set-ups, measurements and validation" provides the reader with the necessary theoretical background, methodology for the experiments and the results of the presented experiments.
- Chapter 5 "Discussion" will discuss both the modelling and measurement experiments. The measurement experiments are linked to the modelling and simulation. The most important findings about the failure mechanisms will be discussed.
- Chapter 6 "Conclusion and Future Work" will provide the limitations and recommendations found after this study. The thesis ends with a conclusion.

2

Background Information

2.1. Balanced Armature Receivers

Balanced armature receivers are electroacoustic transducers that convert an electrical signal into an acoustical signal. The first Balanced Armature technique dates back all the way to 1876 [3] where it was implemented in the telephone. Nowadays balanced armature receivers are widely used worldwide in the hearing aid industry. At the beginning of the 19^{th} century the first variants of hearing aids were introduced in the form of various ear trumpets. This development of technology is divided into five different phases by Volanten [2]. These phases were successively; Ear Trumpets, Carbon hearing instruments, Vacuum tubes, Transistors and Integrated circuits. The final phase, Integrated circuits, started in the 1950's but still is the foundation for the design of hearing aids. On of the most important components of hearing aids in this final phase is the receiver. Volanthen refers to the receiver the heart of the hearing aid.

The general flow of process of hearing aids, is that sound waves arrive and are captured by a microphone. The sounds waves create a pressure difference in the air in the microphone. The change in pressure is converted into electrical signals. These electrical signals are processed by a amplifier and/or DSP (Digital Signal Processor). These processed signals are used to drive the to electroacoustic transducer. In most hearing aids nowadays the type of transducer is a balanced armature receiver. The electrical signals, received by the coil of the balanced armature receiver induce a magnetic flux that causes mechanical movement resulting in an acoustical output.

The Balanced Armature Receiver is popular in the hearing health market due to its size, performance and efficiency. In general most Balanced Armature Receiver nowadays in the the hearing health market vary between 4 mm and 10 mm in length. This small size allows the receiver to be placed at the most distal point of the hearing aid and thus closest to the external auditory canal and auditory system of the ear itself. The performance and efficiency is needed to use the device for longer periods of time without charging.

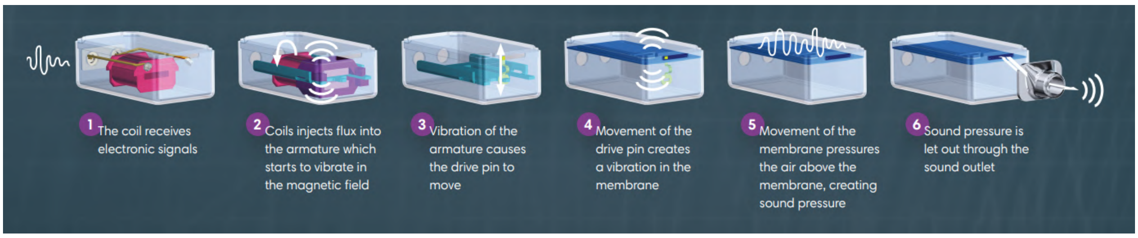

Figure 2.1: Basic principle of a BA receiver, Sonion Balanced Armature Receiver Poster [4]

2.2. The 3100 Balanced Armature Receiver

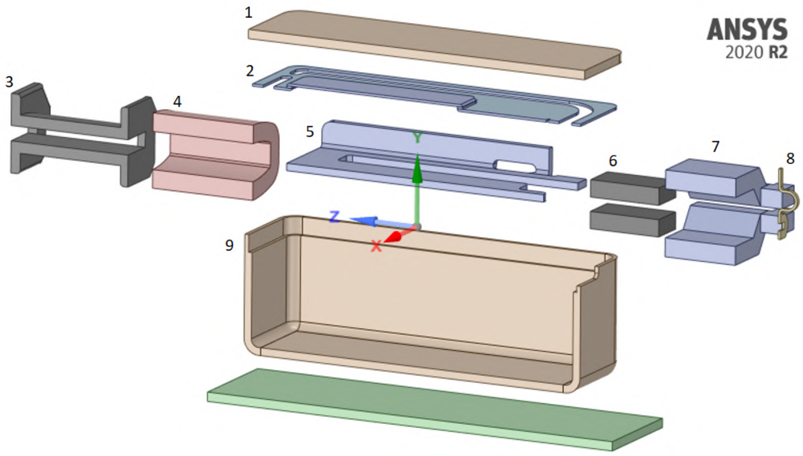

Figure 2.2: Exploded view of a half model of a 3100 balanced armature receiver, Sonion

1. Cover
2. Membrane/diaphragm
3. Bobbin
4. Coil
5. E-shaped Armature
6. Permanent Magnets
7. Magnet Shells
8. Drive Pin
9. Casing

As the name suggest the balanced armature is characterised by the armature (5), which is a beam shaped metal alloy that is balanced between two permanent magnets (6) when there is no current running in the coil (4). The armature is made of a metal alloy, which is a high magnetic permeable material. The geometry can vary in size and shape. In the model shown in fig. 2.2 the armature is called an E-shaped armature. Another well known armature shape is the U-shape armature. Surrounding the armature is a core-less coil (4) that can be excited via a processed electrical signal that usually originates from a microphone and via an amplifier/DSP (Digital Signal Processor). The coil inject a flux into the armature which will vibrate in the magnetic field. The flux on the air gap of one side of the magnets will increase, where as the other will decrease in flux [5]. A force will move the armature out if its balanced position and causes it to move. The armature drives the diaphragm or membrane/diaphragm (2) via a drive pin (8). The motion of the membrane pressures the air in the front volume. The front volume is separated from the back volume by the membrane covered with a foil. The foil has a very small hole to compensate for barometric pressure. The vibrations, and thus pressure changes, in the front volume are perceived by the user as sounds. The back volume, which is the area underneath the membrane adds stiffness to the system. The back volume can either be closed or open (vented), resulting in different stiffness of the system and thus different desired frequency responses.

3
Modelling and Simulation

The body of the thesis will be split up in two chapters which are strongly related to each other. A modelling & simulation part and an experimental part will be written including theory, methodology and multiple experiments. The results of the experiments will be presented in the same chapter, thus modelling results in the modelling and simulation part and measurement and experimental results in the experimental chapter. In both chapters cross references appear to correlate them. Chapter 3 will discuss the different aspects of the modelling and simulation of this research. Starting with Material models that are relevant for this study, then the fundamentals needed for this Finite Element Analysis. The pre-processing, setting up of the model and finally the post-processing steps that are needed for proper analysis. The final part of this chapter before the results is about Virtual Prototyping, different ideas and models are presented. Finally the results will be presented.

3.1. Material Models

This section discuses the most important mechanical and material properties that are needed for a correct model and simulation. Furthermore specific material properties for balanced armature receivers are discussed and the section finishes with an overview of the materials used for the product 3100 balanced armature receiver.

Within the content of this study, material models will contain the material properties that are needed for the desired analysis. For the structural dynamic analysis, such as impact analysis, the mechanical properties will be the most important. Since the balanced armature receiver is a electroacoustic transducer it must be mentioned that for multiphysics analysis it is important to also consider the electromagnetic properties. The main scope of this project mainly focuses on the mechanical properties for the impact analysis in Ansys LS-Dyna. The multiphysics models in COMSOL do include the electromagnetic properties. The COMSOL models include air, as the main interest of these models is to predict the sound pressure output. The material models are one of the most important aspects of a model as incorrect material properties will lead to corrupted results which can not be trusted.

3.1.1. Mechanical Properties

In solid mechanics, mechanical properties define how materials and structures respond to different loading conditions. To calculate the forces, stresses and strains with certain level of accurateness, at least the following properties must be included. Those are density, ρ $[kg/m^3]$, Young's modulus, E $[MPa]$ and Poisson's ratio, υ [-]. With these properties Hooke's law can be calculated and implemented in three dimensions (see equation 3.1). Now linear elastic analysis can be modelled and calculated for most models in the mechanical domain. The three most important properties of the mechanical domain in explicit dynamic analysis are the density, Young's modulus and Poisson's ratio.

Density can be described as the substance mass per unit volume, the SI unit is also therefore $[kg/m^3]$. The density is important for force calculation and inertia. Secondly, the Poison ratio which is based on the ratio of lateral and axial strain. The Poison ratio will show how deformation of a material perpendicular to the applied force/loading takes place [6]. In addition, the Poisson ratio is needed to relate the Shear and Bulk modulus with each other. The third important material property is the Young's Modulus, E $[MPa]$, which is the slope of the linear correlation between stress and strain (see figure 3.1).

$$\begin{aligned}\epsilon_1 &= \frac{1}{E}(\sigma_1 - v\sigma_2 - v\sigma_3) \\ \epsilon_2 &= \frac{1}{E}(-v\sigma_1 + \sigma_2 - v\sigma_3) \\ \epsilon_3 &= \frac{1}{E}(-v\sigma_1 - v\sigma_2 + \sigma_3)\end{aligned} \tag{3.1}$$

It is quite common that studies and papers on drop and shock analysis only include these three properties [7][8]. Seungbae Park *et al.* requires only linear elastic model as the interest in knowing the global dynamic response [9]. The paper of Aishwarya *et al.* includes the yield strength as well [10]. Since the interest of this thesis is also understanding the severity of impact, it is necessary to understand what happens after the yield point. The yield strength is a point at the stress strain curve where the material starts to plastic deform and starts showing non-linear behaviour (see fig 3.1 for a typical stress strain curve of a metal). The consequences of plastic deformation are potential off-sets in one of the components. This deformation can lead to failure or a distorted, unpleasant signal in the output.

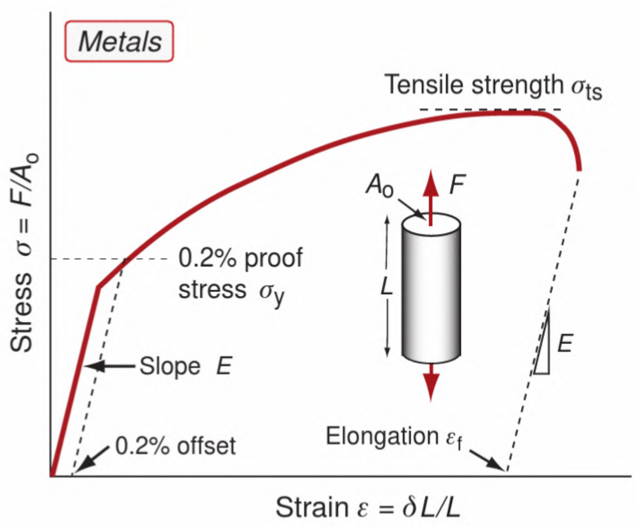

Figure 3.1: Stress strain curve of Metal for the book of Ashby [6]

Non-linearity

Materials can be non-linear in their nature like viscoelastic polymers or simply exceed linear elastic behaviour under severe loading conditions in mechanical analysis. The point of exceeding the elastic behaviour in a stress-strain curve is called the yield point. Drop and shock analysis includes high accelerations, non-linearities and plastic deformations therefor it is important to take into account the behaviour of the nonlinear part of the stress and strain curve. A plasticity model can be implemented in the material models. The plasticity models take into account what happens to the stress strain curve after the yield point has been reached. In comparison with just a non-linear stress-strain curve, a plasticity model takes the in-elasticity into account as well. This means that when a structure is unloaded plastic deformation has occurred. The non-linear stress strain curve that is used for the plasticity model is usually obtained through experimental data. In this study, in Ansys LS-Dyna, the material data of the plasticity model is either implemented as a Bilinear model or as a Multilinear model. Both are a linear approximation of the desired stress-strain curve. The Bilinear curve of the pure nickel originates from the information database Granta, whereas the Multilinear model is based on experimental data from the supplier. In figure 3.2 the Bilinear shows the total Strain (elastic+plastic) and the Multilinear only shows the plastic stress strain relationship.

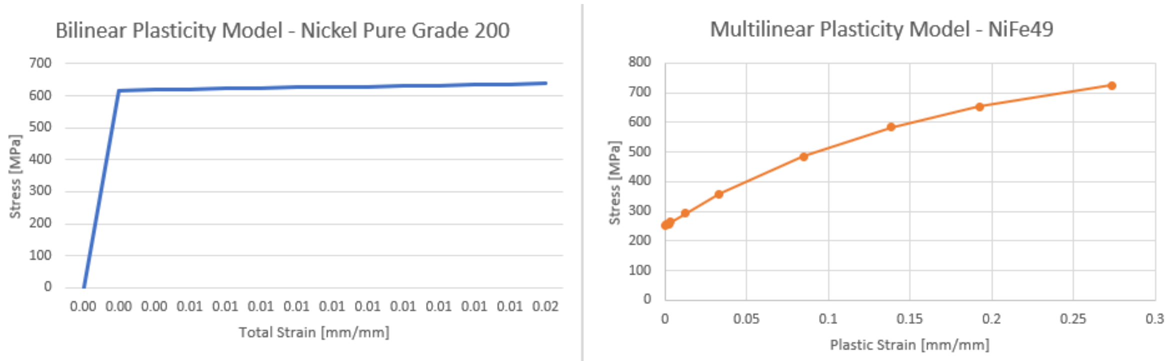

Figure 3.2: Left = The bilinear model for Nickel Pure Grade, Right = The multilinear model for NiFe49

In literature and most comparative research isotropic material properties are most commonly assumed (e.g. [11]). Isotropic material means that the material behaves the same in all directions, $E_x = E_y = E_z$. Living tissue, such as wood, is a well known example that does not show isotropic behaviour but orthotropic (and anisotropic) because of its fibre directions. Anisotropy can also be manipulated by certain processes. For example processing materials, such as rolling metals, can also influence the grain structure, thus modifying the isotropic in anisotropic behaviour. Some of the materials are annealed which might cause anisotropic behaviour, however in this research isotropic behaviour will be assumed for all materials. Most materials are metals and have very isotopic behaviour plus the assumption of isotropic material helps to reduce complexity of the model.

Finally, it is important to understand the scale of your product, a balanced armature receiver is considered still on a macro-scale, approx. a few millimetres. However some components of a balanced armature receiver, such as the armature or membrane, are only fifty to hundred micrometer thick. This thickness might create a situation where the grain sizes of certain metals might influences the behaviour. Again to reduce complexity it is assumed in the models and simulations that this behaviour is not present.

3.1.2. Materials for Balanced Armature Receivers

Balanced armature receivers are electroacoustic transducers, thus most of the materials used must have desired electromagnetic properties as well as good mechanical properties. Therefor the material choice will always be a trade off between desired material properties. When designing a balanced armature receiver the material choice focuses on maximising the desired characteristics of the different components. For example, the membrane must have the precise amount of stiffness to produce the wanted output Frequency Response (FRF). Another example is that it is desirable when designing the armature that the material has a high magnetic relative permeability while having the correct stiffness.

During production, the armature, which is balanced between two permanent magnets, is magnetised. The magnetisation of the armature causes a change in the stiffness behaviour of the armature (see equation 3.2). When the magnetised balanced armature is positioned between two permanent magnets it can experience a force due to the magnetic flux that is caused by the coil that is driven with a certain signal. When the armature is moved out of the balanced position the magnetic field causing one of the permanent magnets to have a higher magnetic force. This phenomenon causes the armature to behave less stiff. This is often referred to as negative stiffness since it creates the tendency for the armature to show more compliance (see equation 3.2). The Magnet shells are also made of high permeable material, in order to guide the magnetic flux back into the armature, closing the magnetic pathway.

$$F_{totalstiffness} = F_{mechanical} + F_{magnetic} = -kx + \alpha x = -(k - \alpha)x \tag{3.2}$$

- k = Positive Stiffness
- x = Displacement
- α = Negative Stiffness

The iron nickel alloys did undergo a special heat treatment called annealing thus a special material model of this alloys must be provided. The data for the material properties of the nickel iron alloys come from Carpenter, which is an external company which provided the test data needed to make the right stress strain curve. It is important to be aware of true stress and true strain. The true stress strain relationship includes the change in cross-sectional area. The data can be found in the appendix B. Sonion Nederland BV has the license to make use of Ansys Granta, which is a material intelligence databases. So the more common material properties can be found on the online Granta material database. In this study materials from the granta database are Nickel Pure Grade 200, AlNiCo magnets and the CuSn6.

In the 3100 balanced armature receiver, as in most receivers, the volume inside can be divided in two separate volumes. The front volume, which is everything above the membrane and the back volume which is the entire volume underneath the membrane. In order to separate the back and front volume a polyurethane foil is placed under tension over the membrane. The foil seals the rails in the membrane. This sealing creates an acoustical stiffness in the back volume. A compensation hole is added in the foil to compensate for the barometric pressure. The size and location mostly affects the low frequencies.

Materials of the 3100 receiver from Sonion

The materials used per receiver model will differ because of desired purposes or innovations that are made. The materials of the 3100 receiver that will be used for this study are listed in table 3.1. Two of the materials, FeNi 49 and nickel pure grade, their plasticity model can be found in fig 3.2. The other models can be found in appendix B.

Component	Material
Casing	FeNi80 - Hymu 80 - Annealed
Cover	FeNi80 - Hymu 80 - Annealed
Armature	FeNi49 - High Permeabillity
Membrane	Nickel Pure Grade 200 (hard)
Magnets	Alnico
Drive Pin	CuSn6
Bobbin	Vectra E130i – LCP-GF30
Coil	FeNi - Copper
Magnet Shell	FeNi49 - High Permeabillity
Foil	Polyurethane

Table 3.1: Materials used per component

3.2. Finite Element Analysis

This section starts with description of the modelling of drop and shock in current studies, the necessary theory behind FEA (Finite Element Analysis) and what will be implemented in this research. This will be followed by the reasoning of what modelling approach will be used for what study. Then the pre-processing steps of a finite element model will be described and explained. The post-processing steps will follow after this. The section finishes with multiple methodologies for different finite element experiments.

The Finite Element Method (FEM) is a method used in computational mechanics and computer aided engineering (CAE) in numerous engineering fields. FEM is a computational method to help solve problems which are too complex to solve analytically. These problems can either be 1D, 2D or 3D. The partial differential equations which arise when solving these physic problems are approximated numerically via discretisation methods. In short, discretisation of the problem means making numerical approximations of the Partial differential equations that describe the problem. Discretisation allows to break the domain of the study in a finite number of elements. In the field of research on impact analysis and structural transient analysis, mostly three dimensional geometries are loaded into FEM solvers. The geometries are often created or prepared in different Computer Aided Design (CAD) programs. Proper preparation of the geometry will include minimising unnecessary details, fixing small holes to properly assign boundaries and if possible making simplifications such as removal of sharp edges. By preparing the geometry correctly, simulation costs will decline and help the solver converge to the correct solution. Finite element models often contain complex geometries and boundary conditions that include different kinds non-linearities. According to the book of Plumbridge, Matela and Westwater there are three major types of non-linearities typically used in engineering problems: Geometric non-linearities, Material non-linearities and Boundary non-linearities [12]. To properly understand and run a model all these challenges with FEA for this research must be tackled.

3.2.1. Modelling of Drop and Shock

In most recent studies finite element modelling and simulation is heavily integrated in the drop and shock impact testing. Modelling drop and shock allows for more insight knowledge to the engineer due to the flexibility of FEA. This flexibility will allow to test and predict various different situations without building and/or damaging the products and the possibility for virtual prototyping. Fast iterations and predictions save costs and time in manufacturing and performing experiments. Besides cost and time efficiency, one of the major advantages of implementing the modelling of the drop and shock loading is the possibility to apply a variety of post-processing techniques which might not possible with conventional experiments. E.g. stress and strain analysis for entire components or energy analysis. The post-processing options allow to better find and study the failure mechanisms of a design.

In transients structural analysis, the dynamic response of a structure under external forces, loads or accelerations, is analysed over time. The equation(s) of motion describe how a structure behaves over time. Analytically, the equation of motion can be seen as one or more Partial Differential Equations (PDE). The finite element method will try and help to solve these complex differential equations. An example in transient analysis, the PDE, a second order differential equation, will have the following form:

$$[M]\{\ddot{u}\} + [C]\{\dot{u}\} + [K]u = \{f\{t\}\} \tag{3.3}$$

M = Mass, $\{\ddot{u}\}$ = Acceleration

C = Damping, $\{\dot{u}\}$ = Velocity

K = Stiffness, $\{u\}$ = Displacement

f = Load, t = Time

For a time dependent FE model there are in general two possibilities for choosing a solver, time integration algorithm, to run a drop and/or shock excitation: an implicit solver or an explicit solver. Appendix A will further explain the analyse technique of the explicit solver used in this study for drop and shock analysis and appendix A will also explain the implicit solver used in this study for the modal and multiphysics analysis. Both solvers offer different numerical methods, each with their own computational characteristics and (dis)advantages. Choosing the right solver for the right transient analysis is essential.

Modelling of a Free Fall Drop Test

The free fall drop test is used very often in different industries and thus also well known in finite element analysis. The objects to drop can vary from very small to larger objects. Oguzhan presented on a conference dedicated to commercialised FEM package LS-DYNA about a drop test simulation of a dishwasher mechanical structure [8] or a LCD screen as presented by Min-Chun *et al.* [13]. The main purpose of those studies is to determine the critical regions in the assembly.

Modelling a free fall drop test is one of the methods that sound relatively straight forward. In this method a direct impact between the balanced armature receiver and the ground would be modelled. To save computational time, the hard surface (ground) is modelled as a rigid body with fixed constraints in all axis and rotations. Initial boundary conditions such as initial velocity (or drop height), contacts and fiction coefficient need to be specified. The FEM used for drop simulation allows to test multiple angles or inclined drop tests with relative ease (see fig 3.3). By choosing the initial position of the drop test, one can save a significant amount of computational time. As argued by Aishwarya Gosavi *et al.* it is recommended to place the "object to drop" as close as possible to the ground and assign a impact velocity [10]. This smart choice of initial position is a perfect example of how one can safe lots computational costs.

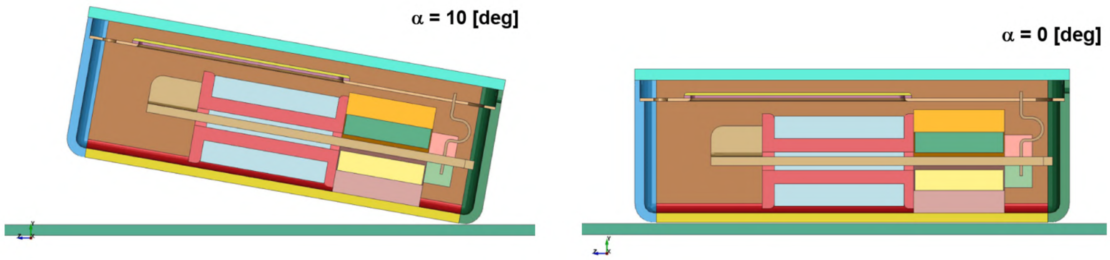

Figure 3.3: Drop test of different angles at the moment of impact, 3100 Receiver of Sonion

Controlled Shock Excitation

There are multiple methods for modelling and simulating controlled shock excitation each with their own characteristics, the most fitting for this study are chosen. The decision of the method must be a balance between maintaining high accurateness and not becoming too computationally expensiveness.

In literature Kamarajan Balakrishnan *et al.* compares the effectiveness of multiple finite element methods for simulation of controlled drop tests of electronic control units [14]. A known method that Kamarajan Balakrishan uses is the Input G method. The Input-G method is often applied in modelling of drop and shock impact tests [15] [14]. In both papers the control unit is fixed with a bonded contact. This is done by either bolts to a drop table or clamped to a test frame. With this method the frame or the bolts are excited with a predefined acceleration. This method saves computational time as it directly puts the acceleration on the bolts and does not require to model the entire table. In literature this method is known to be used with implicit solvers and explicit solvers [14][7]. The support excitation scheme is a technique similar to the input G method and is also discussed by Muthuram *et al.* [7]. This scheme is introduced by Chang *et al.* in his paper, the input acceleration pulse is translated into an effective support excitation load on a test vehicle [16]. Seungbae *et al.* increases the complexity this method and implements the contact behaviour of the bolts in the test set-up as well [9]. The same principle with a different name is applied with the direct enforced acceleration [17].

The large mass method is an alternative method, quite similar to the excitation scheme and input G, that is applied in the modelling of specified acceleration pulses as a base excitation. In the Handbook of material failure, Chapter 7 Analytical solutions for electronic assemblies, the Large Mass Method was used to simulate a base vibration [18]. With this method a model is attached to a very large mass that is several orders of magnitude higher in mass. In this method a fore is applied to the large mass with a known acceleration input. The test vehicle will transfer the desired acceleration loads to the test object. Ahmer *et al.* applies this method as well in his paper [19]. Just as the Input G and Support Excitation Scheme this method can be applied in explicit and implicit analysis and eliminated the need to model the other objects like the drop table and strike surface.

The input G method is tested vs the input G method combined with the Large Mass Method. A simulation is performed where an half sine input force is given in the finite element model. The force input for the model is a function over time dependent on the mass and peak acceleration. Ansys LS-Dyna accept this force input only as tabular data, so a time-step small enough is chosen to capture the function properly. The formula to calculate the input data is as follows:

$$F = m * a * sin(\frac{T * \pi}{dt}) \tag{3.4}$$

F = Force [N]

m = mass of the "large Mass" [kg]

a = Peak acceleration [m/s^2]

T = Time [s]

dt = Time Step [s]

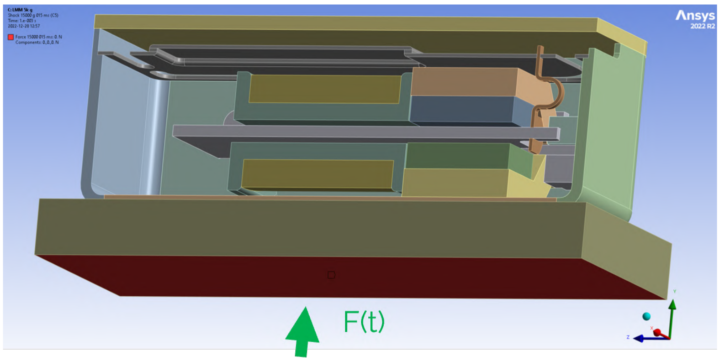

Figure 3.4: The Force is applied at the bottom.

For these small experiments a acceleration with a peak of 15.000 [g] and a duration of 0.5 [ms] is used as input (see figure 3.4). It is common in this field of research to use g as terms of expressing acceleration. 1[g] = 9.81 [m/s^2]. With the post-processing software LS-PrePost the acceleration at the bottom part of the receiver and the armature are extracted. These are plotted against each other to see which method gives the most control on the acceleration of the armature, see fig 3.7 and fig 3.8.

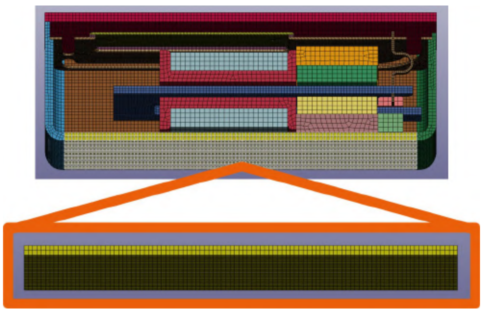

Figure 3.5: Acceleration bottom of the receiver

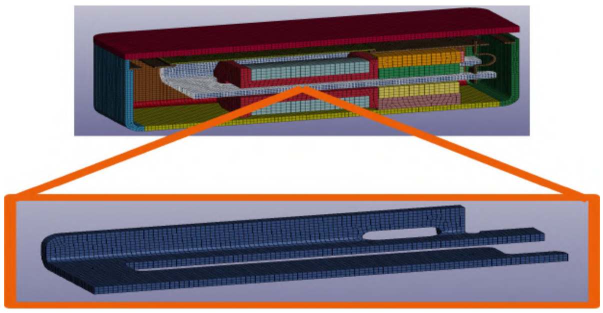

Figure 3.6: Acceleration armature of the receiver

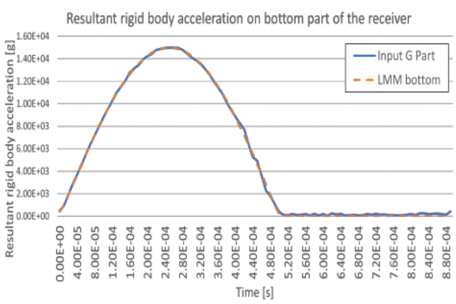

Figure 3.7: Acceleration bottom of the receiver

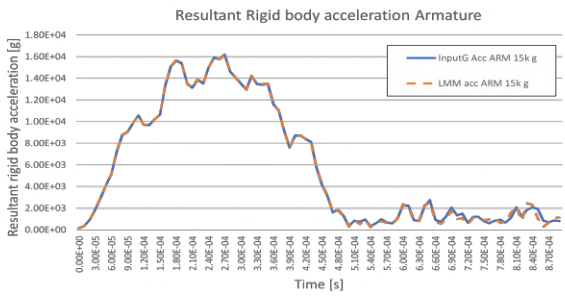

Figure 3.8: Acceleration armature of the receiver

As can be seen they both produce very similar results. A combination of LMM and Input G is applied in this study. An advantage is that the input is applied directly at what would be the pendulum head (in experimental set-up) and the large mass better simulates the situation of the test set-up where the receiver is mounted to this pendulum head. Further information on the test set-up can be found in section 4.2.1.

FEA Software and Solvers

In this study the explicit simulation software Ansys LS-Dyna is used for the impact analysis. The explicit solver of this software is widely used and preferable for these kind of impact time-dependent simulations. Mostly because of its robustness and capabilities to solve highly non-linear problems. The multiphysics software from COMSOL is used for modal and multiphysics analysis. These studies are frequency dependent studies and therefor no time integration solver is needed for these steps.

Explicit finite element method is very efficient in short-duration problems in nonlinear structural dynamics [20]. Such events can involve shock waves, high impact velocities and explosive blasts. Numerical drop impact analysis is mostly carried out by using an explicit solver. Explicit time integration uses the slope at known step to find the next solution (see equation 3.6). One of the most commonly used time integration methods in explicit analysis is the Central Difference Method. A more detailed explanation of explicit solvers and The Central Difference Method can be found in the appendix A. A overview of the most used explicit software are presented in table 3.2. More information on implicit time integration solvers can be found in appendix A.

$$\frac{dy}{dt} = f(t, y) \tag{3.5}$$

$$y_{k+1} = y_k + hf(t_k, y_k) \tag{3.6}$$

Explicit FEM Software	**Literature**
PAM-CRASH	Kim Low *et al.* [21] Solanki *et al.*[22]
Ansys LS-DYNA	Seungbae Park *et al.*[9]
Ansys Explicit Workbench	Aishwarya Gosavi *et al.* [10]
Abaqus Explicit	JingJing Wen *et al.* [23]

Table 3.2: Overview Explicit Solvers

In order to achieve stability with explicit solvers, the size of the time-step is limited [20]. The stable time step formulation, called the Courant-Friedrichs-Lewy condition (see eq. 5) is a convergence condition for explicit time integration schemes. A technique that is often used to increase the time step is call Mass scaling [20]. Hereby nonphysical mass is added to gain a larger explicit time step. Increase of density leads to a smaller wave speed in the material which equivalently means a larger time step. When setting up the simulation in Ansys LS-Dyna there is a simple setting which allows the time scaling option to "yes".

$$\Delta t \leq k_{min} * \left(\frac{l}{c}\right) \tag{3.7}$$

Δt = Time-step

l = Characteristic length of a finite element

c = Wave speed in a material ($c = \sqrt{\frac{E}{\rho}}$), E = Young's modulus, ρ = Density

k_{min} = Safety factor

Overview of Different Software used

After the literature study and exploratory research it has been concluded that the following software packages will be used in this study. Spaceclaim, see section 3.2.2 for further explanation, will be used for pre-processing of the CAD geometries. LS-PrePost will be used for post-processing of the results. Ansys LS-Dyna will be used for setting up, running and solving the drop and shock models and simulations. COMSOL will be used for modal analysis of the balanced armature receiver. COMSOL multiphysic analysis will be done to perform a fully coupled multiphysics simulations which will be implemented to see the effects of certain changes on the FRF output.

- Ansys® Spaceclaim
- Ansys® LS-Dyna
- LS-PrePost
- COMSOl Multiphysics®

3.2.2. Pre-Processing of the Finite Element Model

Geometry Input

Sonion has produced and developed multiple balanced armature receivers, the product used in this study is the 3100 series, the model 31A007G is used. In order to optimise the finite element model, it is important to prepare the 3D geometry CAD file before meshing and running the model. Features that are not necessary to obtain a better understanding of the failure mechanisms of the receiver are to be removed with the help of CAD software. In this thesis CAD programs Spaceclaim and Solidworks are used. For the geometry of the 3100 the preparation includes removal of the wiring, any writing (name, model number etc.), the connection plate and spout. When the design is presented from the drawing engineer it usually contains lot of details or margins/off-sets which are no problem for the 3D drawing itself, however it can cause problems with meshing and cause large computational times or wrong results. Intersection and very small gaps need to be removed. Very thin edges or sharp corners can be simplified with CAD software tools to speed up the simulation and improve mesh quality. Simplifying should always be done with care, since you don't want to oversimplify your model.

In Ansys LS-Dyna the bodies of a structure can either be defined as a flexible body or as a rigid body. A flexible body allows for deformation, while a rigid body does not deform under any stress. To define a rigid body, only the density properties must be defined since it will calculate the mass and inertia [24]. If a body is much stiffer than the rest of the structure and deformation is of less interest it can be beneficial to assume this as a rigid body. All the parts of the balanced armature receiver will be considered flexible, however certain carriers which represent a test set-up can be considered a rigid body. This will save computational time and allows for certain rigid body constraints.

Finally, applying symmetry conditions can be performed as part of the pre-processing process. Symmetry conditions are a function that is widely used in finite element analysis. If the model has a symmetric plane or cross-section and symmetric loading conditions, it is possible to apply planar symmetry. By applying symmetry conditions the computational time and required memory is reduced significantly. The 3100 receiver has the possibility to apply a symmetry plane, therefor the symmetry condition will be implemented, thus most of the figures which present the FE model will be a cross-section.

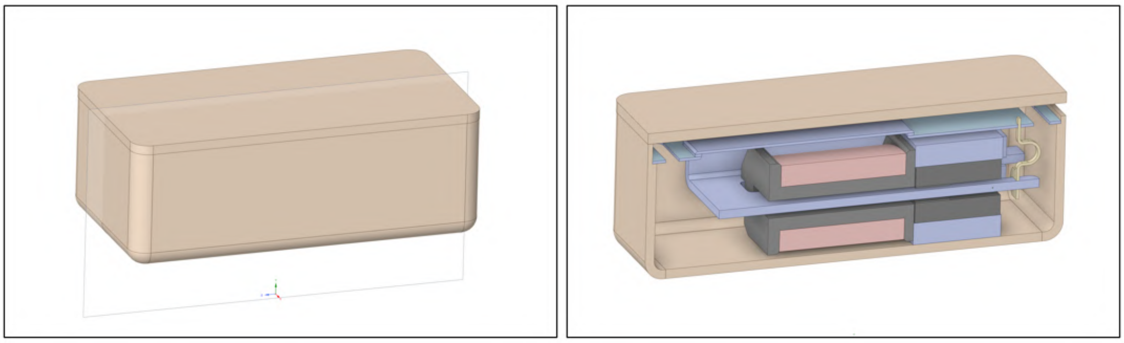

Figure 3.9: Applied Symmetry plane

Meshing and Element choice

Meshing a 3D geometry means discretising the geometry in a finite number of elements with nodes and coordinates that represent the geometry. Once properly prepared, the geometry of the balanced armature receiver model is meshed into a number of finite elements and nodes. There are two important considerations which define the choice of the elements used for meshing. The best type of element suitable for the solution and the mesh size. A good mesh defines the accuracy and the computational time of your simulation. A good way to classify the elements is by geometrical dimensions, 1D, 2D and 3D. These element geometries are often referred to as Beam, Shell and Solid. In general the order of the elements are either linear of quadratic. In explicit dynamic analysis the element order must be set to Linear [24]. The explicit simulation in Ansys will be Hex-dominant. In Comsol the mesh will be mostly a tetrahedral dominant mesh.

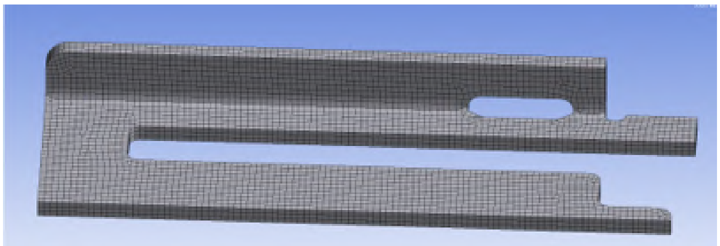

Figure 3.10: Meshed Armature in Ansys, meshed with Hex Dominant Elements

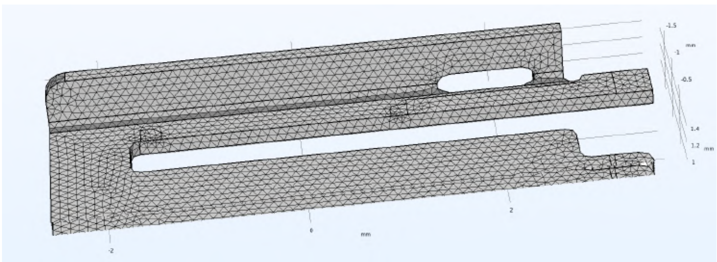

Figure 3.11: Meshed Armature in Comsol, meshed with Tetrahedral Elements

The size of elements is dependent on the geometry of the part, contact regions and the region of interest. For explicit analysis the minimum thickness should at least be 2 element to capture the stresses properly. The Ansys LS-Dyna simulation produces the best results if the mesh is as uniform as possible. The tetrahedral mesh in Comsol should also be more fine in the region of interest. Most of the time a finer mesh is will capturing the behaviour of physics better as it mostly produces more accurate results. A trade-off is that a finer mesh will results in more computational time and power.

In numerous modelling and simulation studies a combination of solid and shell elements are just, e.g. the study of Luo *et al.* [11]. Since the membrane is very thin, shell element might be a possibility to use for this component. With the Spaceclaim CAD software the geometry is made suitable for the use of shell elements. However after running the simulation with the membrane as shell elements it became clear that the elements were not as good as capturing the proper stresses and strains as two layers of solid elements. Thus it was chosen to keep using only solid elements.

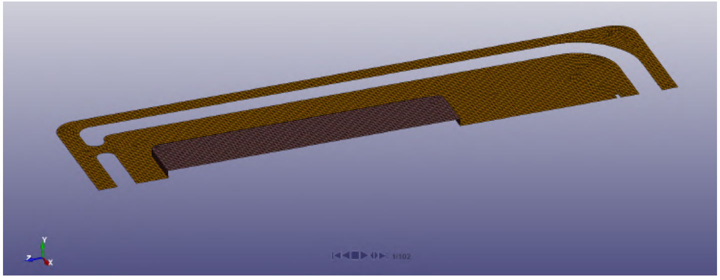

Figure 3.12: The membrane with the use of shell elements

Damping

Damping is often referred to as the dissipation of energy. In different physics, different multiple types damping work in parallel, however three most known types of damping in engineering known are viscous, material and frictional damping. Implementing damping in a FE model can be of great influence of the performance of your model. Different types of damping might be relevant for different kinds of analysis. Modelling transient analysis with an explicit solver, the damping often is taken into account via contacts and material properties. Therefor when performing explicit non-linear analysis it is important to have non-linear material properties, such as plasticity models which include the energy that is needed for plastic deformation. With impact analysis the energy is as also dissipated via the contacts and friction that occurs between different parts. Ansys LS-Dyna offer to artificially add numerical damping in the form of Rayleigh damping. Which is well known numerical type of applying damping in a model, it is a linear combination of the stiffness damping and the mass [25]. However it is unlikely that this type of damping is implemented in explicit impact analysis.

Constraints and Contact

When building any type of model one should be aware to properly add constraints. If you leave out any constraints the amount of degrees of freedom becomes to much and the model will never converge to a proper solution. Over-constrain the model and the solution will not be realistic, for example restricting all translation or rotation in a certain direction.

Proper constraints can be used to exclude parts of the geometry. For the most important components, the armature and the membrane, it is of interest to look at the eigenfrequency analysis. Instead of modelling the entire model, which takes up large amount of unnecessary computational time and memory. It is better to put fixed constraints on the locations where e.g. the armature is fixed. This way the remaining geometry does have to be meshed and calculated but does the simulation remain realistic.

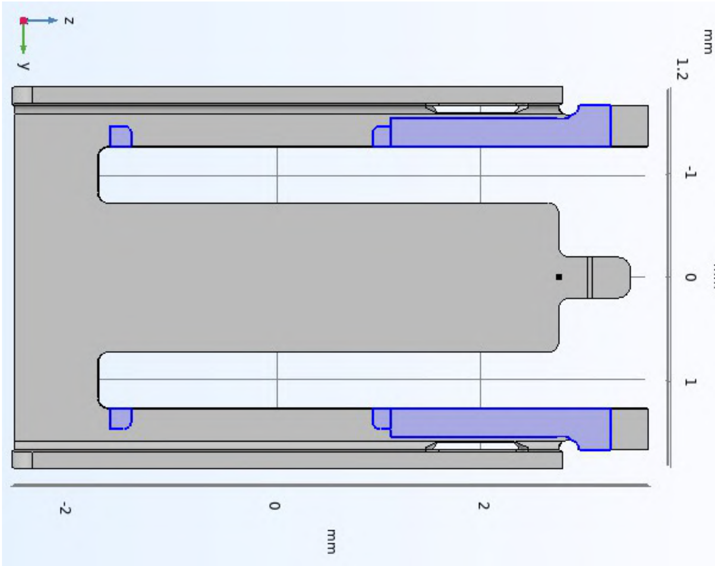

Figure 3.13: By constraining the correct boundaries, computation effort can be saved while being accurate

The structure of the model contains multiple components, which are in contact with each other or might become in contact with each other. Ansys LS-Dyna uses a penalty function to define the contacts. The contact or penetration can be visualised as a very stiff spring. As soon as the solver solution detects the penetration, the "spring" will exert a force to counter the penetration. Much like how real contacts work.

Every contact in finite element analysis between two (or more) structures must have a master and a slave. In the Ansys environment this is called contact and target. From now on contact and target will be used as terminology. In general the rule of thumb for choosing the contact or target side is as follows. The contact side is mostly the side that:

1. Assign the contact side to the surface with a finer mesh
2. Convex shape as contact side, flat or concave shape as target side
3. Soft material as contact side

Based on the rules of thumb it follows that the element size difference between two parts in contact must not be too large in order to properly calculate the physics of the contact region. The boundary conditions of the contact must also be specified, for example the amount of degree of freedom. In the case of fig 3.14 it will be a fixed contact.

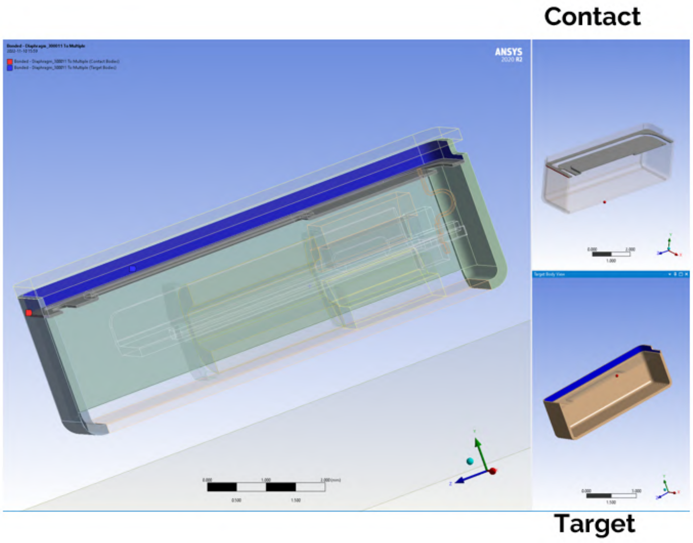

Figure 3.14: One of the defined contacts in the model is the contact between the membrane and the casing

A sub-section of the contacts are called the "body interactions" in Ansys LS-Dyna. These are regions of different parts that might be in contact with each other over the period of time. An example is the armature hitting the magnets after the shock excitation. As soon as contact is detected, the penalty formulation is again applied.

Analysis Settings

In the explicit solver Ansys LS-Dyna there are a few settings which are important and must be well defined before running the simulation. Obviously the end time must be given, which will be set on 1ms for most of the simulations in this study. To reduce the run-time Mass Scaling must be set to "yes". The added mass must be checked after the simulation to check if this is as low as possible (no more than 5%, preferably lower) so it does not influence the physics too much. The time step must be determined, since with explicit analysis the time step is dependent on the size of the element, a CFL time step can be calculated (built in function of Ansys LS-Dyna). It is advised to use this value as guideline. Furthermore the amount CPU's must be set to 4, this is dependent on the license you have and the amount of memory allocation. The history output can also be manually set to a desired amount of data points which is 560 MB in this case. The hourglass type is set to Belytschko-Bindeman which is most preferable for the type of analysis in this study. Furthermore the output controls must be set to desired options.

3.2.3. Post-processing of the Finite Element Model

Energy

Making sure that the energy balance is correct is probably the first important step to check if your explicit FE model is correct. The total energy of a system must be constant over time unless work is added. In this study there is a rise in energy during the force input. Figure 3.15 shows what the total energy function looks like. The energy analysis is also a powerful tool in the post processing of your model, this can either be to check the quality of your model numerically, but also help with understanding the physics behind the failure analysis. A complete energy check can be found in appendix C, the two most important energy checks in this study are the hourglass energy and the internal energy.

The energy balance defined by LS-Dyna is "$totalenergy = internalenergy + externalwork$", or in other words [24].

$$\frac{Totalenergy}{(internalenergy + externalwork} = 1 \tag{3.8}$$

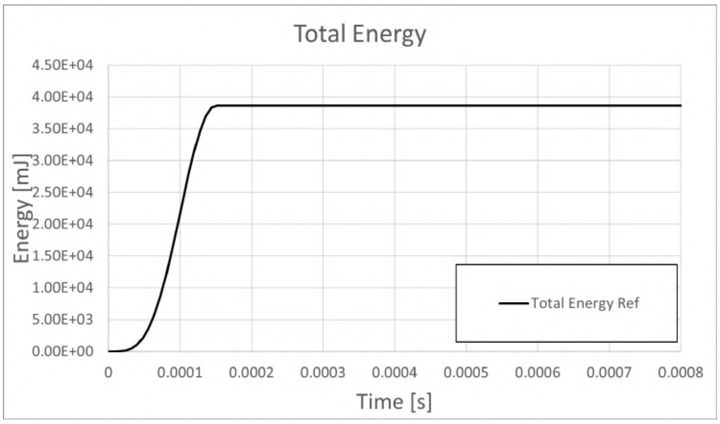

Figure 3.15: Total energy of the entire system during shock

Hourglass Energy

Hourglass Energy is a numerical phenomenon what happens when an element is under-integrated see fig 3.16. The hourglass modes will have zero stress and zero strain. The hourglass modes will lead to large deformation since there is no resistance from the element. In order to control the hourglass modes forces are added to an element to resist the hourglass mode [20]. Adding these forces will require Energy. It is desirable when running a simulation to keep the hourglass energy as low as possible relative to the internal and kinetic energy, since these forces are purely numerical. Ansys LS-Dyna includes the hourglass energy in the internal energy, therefor both should be plotted and compared with each other.

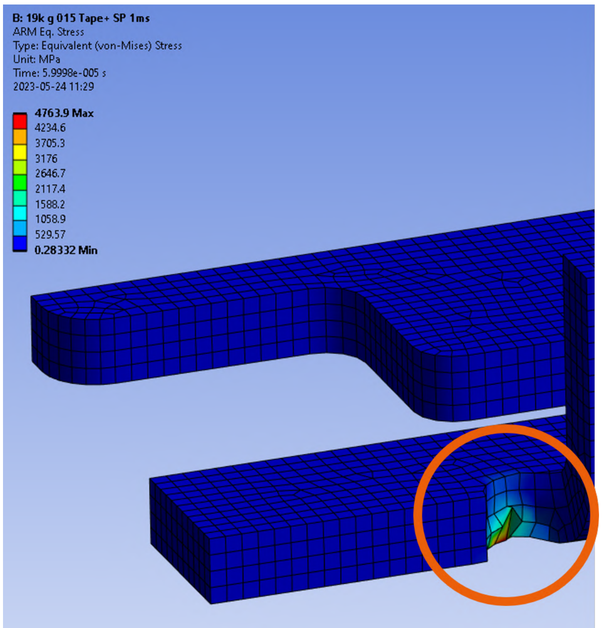

Figure 3.16: Hourglassing of under-integrated elements in the armature hinge.

Internal Energy

Internal Energy in impact analysis is defined by Ansys LS-Dyna as "the energy stored due to deformation". The energy stored due to deformation is directly linked to stresses and strains, see equation 3.9. The Internal energy is a good approach to make a global assessment of the response of the structure, specially for comparing different designs or testing scenarios. The internal energy can be analysed per component instead of a stress distribution, which is more focused on local regions and can be more difficult to quickly asses. This deformation can either be due to permanent deformation, which is often called inelastic strain energy or plastic strain energy, but also includes elastic deformation. This means that the internal energy includes the elastic strain energy and the inelastic strain, however it also includes the hourglass energy. Thus it makes sense that the hourglass energy is kept to a minimum. In Ansys LS –DYNA the internal energy is calculated incrementally for each element as follows:

$$(IE)new = (IE)\,old + sum\ over\ all\ six\ directions\ of\ (stress * incremental\ strain * volume) \quad (3.9)$$

$$(IE)new = (IE)\,old + sum\ over\ all\ six\ directions\ of\ (\sigma * \epsilon * V) \quad (3.10)$$

The elements are summed to give the total amount of internal energy. High values usually indicates (plastic) deformation which is related to high stresses. When protecting a certain component, the amount of energy due to deformation must be minimised. The internal energy per component gives insight to how energy is dissipated within the structure.

Von Mises Stress

High stresses often arise in critical region of a design. Stress analysis will give insight in where and how severe these critical regions are under certain loading conditions. The von Mises stress is widely used to determine if a material, usually a ductile material like metal, will yield or fracture. The von Mises stress is an equivalent stress calculated through the principle stresses (or stress tensor). The equivalent von Mises stress is calculated over multi-axial loading. If isotropic behaviour is assumed it allows the engineer to compare failure mechanism with simple tensile test information.

$$\begin{bmatrix} \sigma_{xx} & \sigma_{xy} & \sigma_{xz} \\ \sigma_{yx} & \sigma_{yy} & \sigma_{yz} \\ \sigma_{zx} & \sigma_{zy} & \sigma_{zz} \end{bmatrix}$$

$$\sigma_v = \sqrt{\frac{(\sigma_{xx} - \sigma_{yy})^2 + (\sigma_{yy} - \sigma_{zz})^2 + (\sigma_{zz} - \sigma_{xx})^2 + 6(\sigma_{xy}^2 + \sigma_{yz}^2 + \sigma_{zx}^2)}{2}} \quad (3.11)$$

Strain

Strain is the response, change of shape, of a structure to its loading and stresses it experiences [6]. Strain can be categorised into elastic strain and plastic strain. Elastic strain will deform back to its original state. Plastic strain occurs when the stresses exceed the elastic modulus, thus plastic deformation. The strains in the results and the Post processing software of LS-Dyna are true strains. True stress and strain take the change in cross section and length into account, thus being more realistic. To collect the data to analyse the plastic strain, the probe for EPS (Effective Plastic Strain) must be inserted in the Ansys LS-Dyna model. The reason the plastic strain and plastic deformation is so important is that this will lead to off-sets that will influence the performance and distortion of the balanced armature receiver.

3.2.4. Orientation

The orientation of the balanced armature receiver can heavily influence the response of the structure. To better understand the failure under shock loading, is it of interest to find the most severe orientation and gain insight in how this orientation influences the response. It is to be expected that a force or acceleration perpendicular to the armature and membrane will cause the largest bending moment and thus the highest stresses. In all the receiver models in Ansys LS-Dyna the top and bottom will always be perpendicular to the Y-axis. So orientation A has the cover to the positive Y-direction and orientation B the bottom to the positive Y-direction.

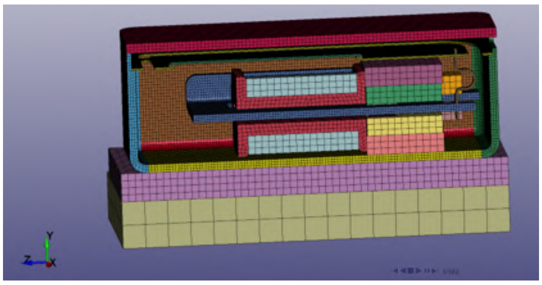

Figure 3.17: Orientation A

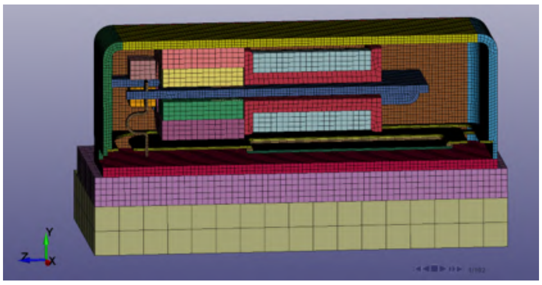

Figure 3.18: Orientation B

Two orientations will be modelled, bottom down (orientation A) and bottom up (rotated 180°) (orientation B). All the other parameters and input will be kept constant. These two orientations are also standard orientations in the regular failure tests within Sonion. In figure 3.17 en 3.18 the lowest block (yellow) represents the pendulum head and the one above it (pink) the double sided M3 tape that is used to mount the receiver to the shock tester.

3.2.5. Shock Waveform

Literature has shown that applying a half sine as idealised waveform has been done and is quite common in modelling of drop and shock. Section 4.2.8 provides information and validation of the shock waveform that is experienced by the shock tester at Sonion. However it provides knowledge insight in the behaviour of the model to compare different levels of shock excitation. In literature mostly a duration of 0.5 ms is the standard, the measurement in section 4.2.1 indicates a duration of 0.15 ms. The idealised half sine make it easy to test different simulation with a different duration, while keeping the magnitude/amplitude the same.

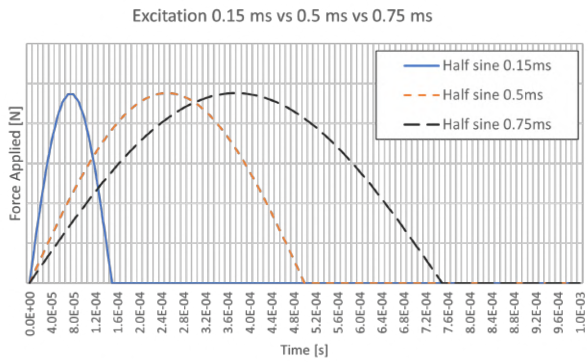

Figure 3.19: Three half sine pulses as an input

Since the test equipment used in this thesis are measured to be 0.15ms all the inputs for the FE models will stick to this value. Most simulations will have a shock amplitude of the highest value possible on the shock tester in the lab. This is 19.000 [g] (see section 4.2.1).

3.3. Virtual Prototyping

In this section different aspects of virtual prototyping in regard to this project are discussed. In the balanced armature receiver there are two main components which are the most prone to damage and arguably the most important for the performance. To improve the robustness of the balanced armature receiver the focus should be on what can be done around the critical areas of these components. With the help of virtual prototyping predictions can be made to see what adaptations can increase this robustness. The focus can either be on protecting the armature, which is forced out of the balanced position and hits the magnets due to shock. Or the focus can be on increasing the stiffness of the membrane which is sensitive to high accelerations. Specially altering the stiffness of the membrane can influence the performance of the receiver. In order to make a proper prediction of the consequences of making the balanced armature more robust, a fully coupled COMSOL model will be made next to the Ansys LS-Dyna models used for impact analysis. Fully coupled indicates that the simulation is a multiphysics simulation where the receiver (the coil) is driven with a nominal voltage drive resulting in a prediction of the FRF of the sound output. The reference model in COMSOL will be validated via the measurements in section 4.2.8. From this point the different designs of the membrane can be modelled as well.

3.3.1. Shock Protection Armature

In order to protect the armature against high stresses and potential damage, shock protection can be added in the form of shock plates. The hinges in the armature experience high stresses if the armature has a large bending moment. To reduce the force and bending moment shock plates are added between the armature and magnets. Different material designs ideas will be presented:

1. Option 1 - Shock plates, made from Nickel Sulfamate
2. Option 2 - Shock plates, made from Rubber Nitrile

Option 1

In order to restrict the maximum displacement at the end of the armature and thus reduce the amount of stress, plates can be added. The shock plates are two very small cylinders located between the magnets and the armature. The plates must limit the maximum displacement while dissipating the energy as good as possible, therefor limiting the amount of mechanical damage done to the armature. The first option for the shock dampers are made of Nickel Sulfamate.

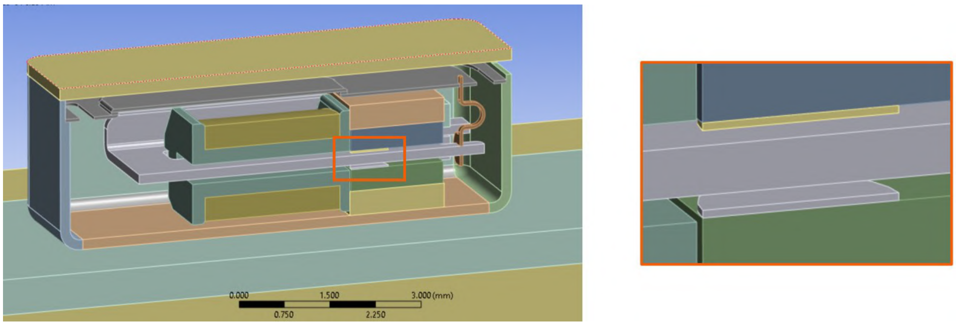

Figure 3.20: Shock plates made of Nickel Sulfamate.

Option 2

A different material is chosen for the shock plates, a material that has better properties to absorb/dissipate the energy. Nitrile rubber is chosen, based on the findings of the paper from Andrzej Grzadziela and Marcin Kluczyk [26]. This rubber has the lowest rebound in their test and would be most suitable for protection of the armature without creating a large rebound effect after impact.

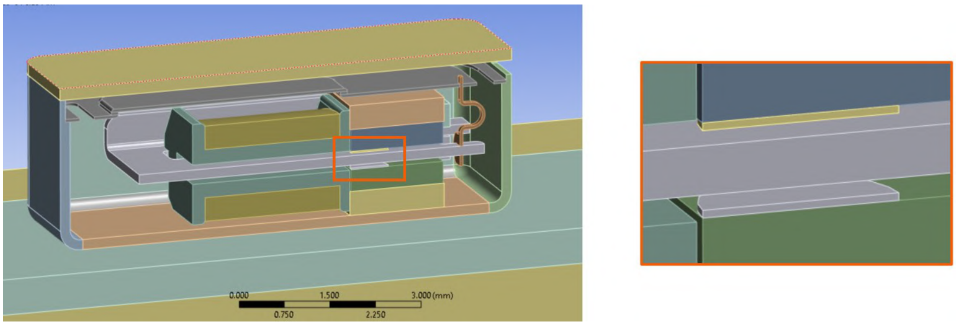

Figure 3.21: Shock plates made of Rubber Niltrile

Both designs try to restrict the amount displacement the armature can have reducing the impact of the shock, without limiting the performance of the armature itself. The designs intend to give an better insight on how fast virtual prototyping that can be implemented using the methods of Finite Element Analysis. Expected is a difference in the response of the armature. The membrane is expected not to be influenced much by the changes.

3.3.2. Changing the stiffness of the membrane

The current design of the membrane has an thickness of 50 μm and an embossed area, which provides the membrane with more stiffness. In order to better understand how the stiffness and design contribute to the robustness two different adaptations are made to the membrane. One design will be a more compliant membrane and the other one has an increased stiffness. Thus the two modelling experiments will show how changing the stiffness will influence the robustness.

It should be noted that changing stiffness and design in the membrane will lead to different FRF in the output of the balanced armature receivers. The simulation experiments in Ansys LS-Dyna are done to highlight the mechanical effects and potential improvements for robustness of the membrane under shock loading condition. The modelling experiments in COMSOL Multiphysics are done to study the effect of these adaptations on the output. Option 1 is a more compliant design, where the thickness is kept the same over the entire membrane. The embossed area is removed, thus decreasing the stiffness behaviour. Option 2 has the stiffness increased by thickening the membrane as well as the embossed area. Since the shock plate designs barely have any influence on the response of the armature, the different models include the Nickel Shock Plates.

1. Design 1 - Removal of the embossed area - flat membrane. The entire thickness is evenly distributed and has now a thickness of 50 μm.

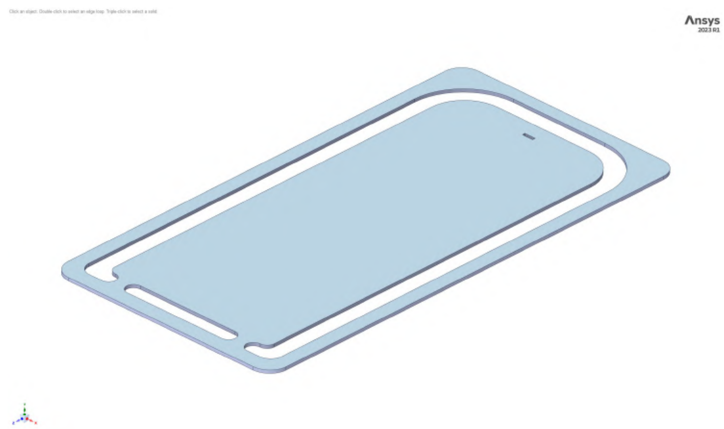

Figure 3.22: Design 1: Removal of the embossed area

2. Design 2 - Increasing the overall thickness of the membrane. The membrane is increase with 50 μm, the results is an overall thickness of 100 μm across the membrane. The height of the embossed area is still 50 μm.

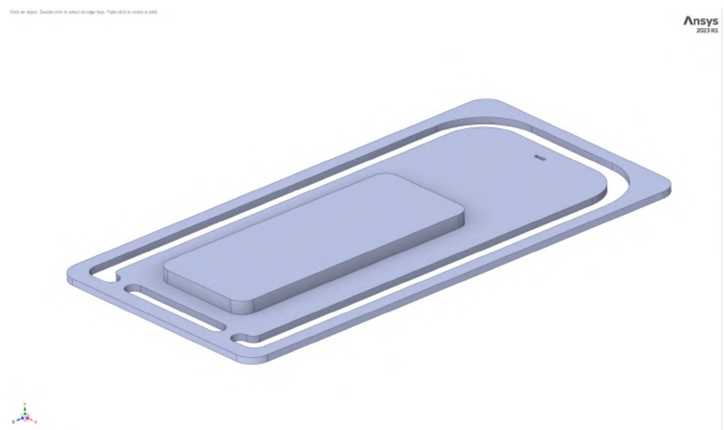

Figure 3.23: Design 2: Increasing the stiffness of the Membrane

3.3.3. Fully Coupled Model - COMSOL

To understand the effects of changing the stiffness a fully coupled multiphysics model is made in COMSOL. First a reference model must be made, this fully coupled model is modelled to simulate the dBSPL measurements in section 4.2.8. This means nominal drive of 110 mV RMS using, ITE (In The Ear) tubing and a 2cc Coupler. More explanation on this can be found in section 4.2.8. The output that is of most interest is the FRF of the dBSPL output. With COMSOL visualisation of the pressure distribution can be made to help better understand the frequency response and the eigenfrequency. E.g. if a peak in the response is mechanically dominated by for example the eigenfrequency of the motor (armature+drive pin+membrane) or is acoustically dominated. Understanding the behaviour will also help understanding how changing the stiffness influence the sound output.

The preparation of the 3D geometry of the model is essentially the same as preparing it for a shock simulation. This time the foil however is implemented to properly model the FRF. The rails, which are usually covered by the foil are now set-up with a cap function with slip condition in COMSOL. The rails are the open space on the membrane. Capping this means no air is able to travel from the back volume to the front just as if the foil was in place. The slip condition allows for proper prediction of expected behaviour. A coil geometry analysis must be performed, in order that COMSOL knows how to properly implement the homogenised coil in the electromagnetic coupling. The values for driving the receiver are the same as in the experiment in section 4.2.8. The mechanical material properties are the same as in the Ansys LS-Dyna model, however a plasticity model is not necessary for this type of analysis. The electromagnetic properties such as relative permeability, measured BH-curves from Sonion to capture the magnetic properties and air needs to be defined to properly capture all the physics. The mesh of the COMSOL model is tetrahedral dominated to capture the complex geometry properly. With the correct multiphysic couplings the sound pressure output can be simulated with enough accuracy to analyse the consequences of altering the design.

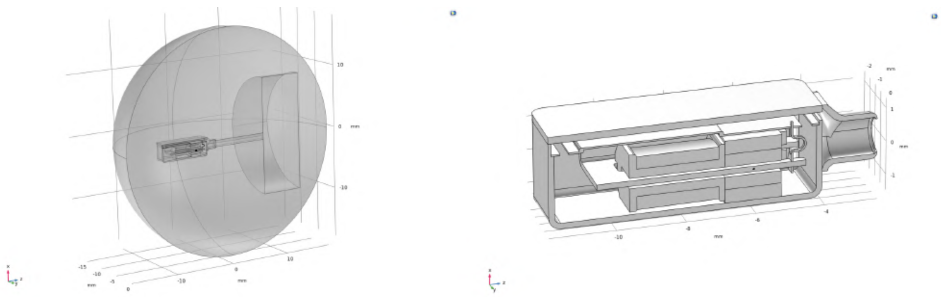

Figure 3.24: Left: Receiver including magnetic and air domains, Right: Receiver only (both with symmetry conditions applied)

The changed membranes are imported in the reference COMSOl® multiphysics model. Making sure all the boundary conditions are consistent. The other simulations can be made to show the effects of the changes in the membrane.

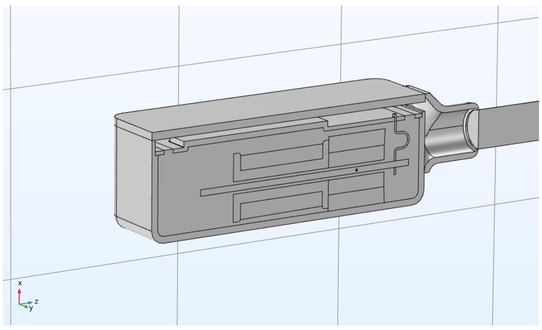

Figure 3.25: The Geometry including the 100 micrometer thick membrane prepared and ready for the simulation

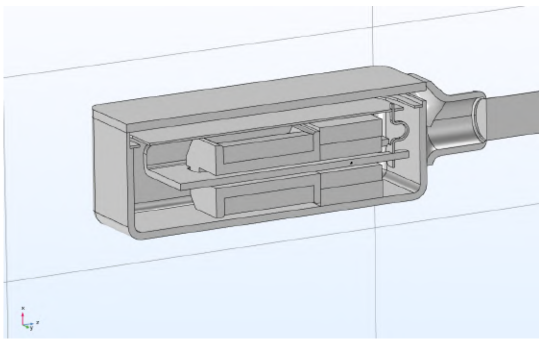

Figure 3.26: The Geometry including the membrane without embossment prepared and ready for the simulation

3.4. Modelling Results

This section presents the results of different models and computer aided experiments. The results are presented and the observations are described. The most interesting mode shapes of the armature are presented first. An energy check of the build reference model is presented. The results of an implementation of tape used by the experiments are provided. Then the reference model is compared with a model with Shock plates. The consequence of the orientation are also presented. The results of shock models and the multiphysic model of the membrane alterations are presented. Finally a final off-set approximation of the membrane is presented.

3.4.1. Modal Analysis

In order to determine the mode shapes of the armature of the receiver, it is given a fixed boundary condition similar when it is mounted within the balanced armature receiver see fig 3.13. An eigenfrequency analysis is done by COMSOL which will give the following mode shapes (see fig 3.27). These mode shapes are purely mechanical, any influence of acoustic pressure is left out since the validation measurement are also open motor.

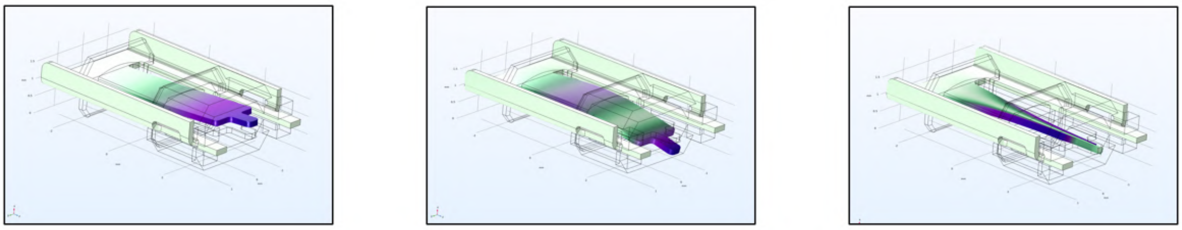

Figure 3.27: First mode shape is at 3446 Hz, second mode shape is at 21397 Hz, third mode shape is at 28650 Hz

3.4.2. Energy Check

Before being able to properly check any results the user must check the energy ratio, added mass, unexpected rise of energy and hourglass energy compared to internal energy. An example of the hourglass check in the armature is given in fig 3.28, a complete overview of the multiple energy checks can be found in appendix C. Hourglass energy is explained in section 3.2.3. The rule of thumb is no more than 10 % to have a reliable model. The added mass must always be as low as possible as well, preferably less than 5 %. The model that is made to be the reference model has a hourglass energy of less than 1 % of the total internal energy.

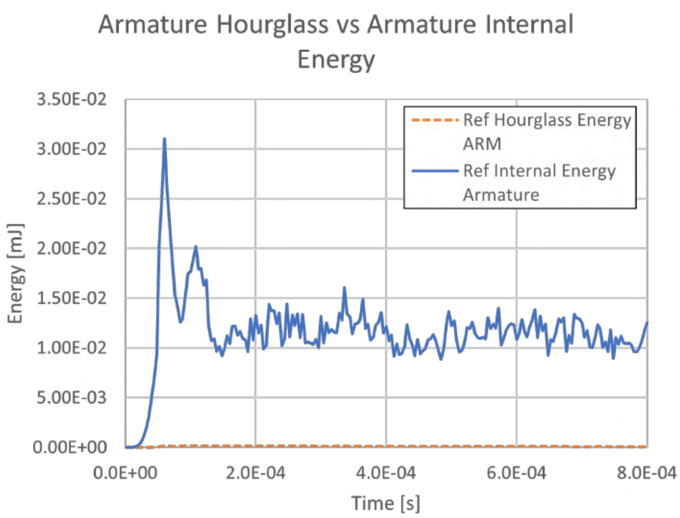

Figure 3.28: The Hourglass is kept at a minimal.

3.4.3. Tape

In the experimental test set-up the balanced armature receivers are mounted to the pendulum swing (for more info about the measurement set-up see 4.2.1) with double sided VHB tape, from 3M. Thanks to the courtesy of the company of 3M it was possible to implement the proper material model for the material. To test the influence of this tape, a comparison is made between including the 3M tape which mounts the receiver vs without. In figure 3.29 and 3.30 the acceleration of the bottom of the receiver and the acceleration of the armature are compared after a shock excitation of 15000 [g]. It can be seen that implementation of the tape slightly influences the response. However the tape will be included in further experiments since the difference is noticeable and closer mimics the real test set-up.

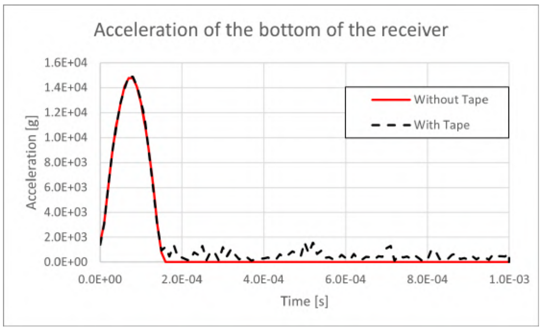

Figure 3.29: Bottom

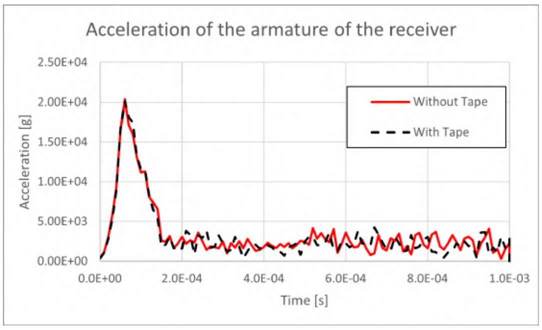

Figure 3.30: Armature

3.4.4. Orientation

Comparison is made between the orientation, 180 degrees around the z-axis, of the receiver (see fig 3.17 and 3.18). All the boundary conditions are kept constant, only the orientation is different.

The internal energy stored due to deformation in the armature is almost similar. The orientation of the receiver appears to have little effect on the armature.

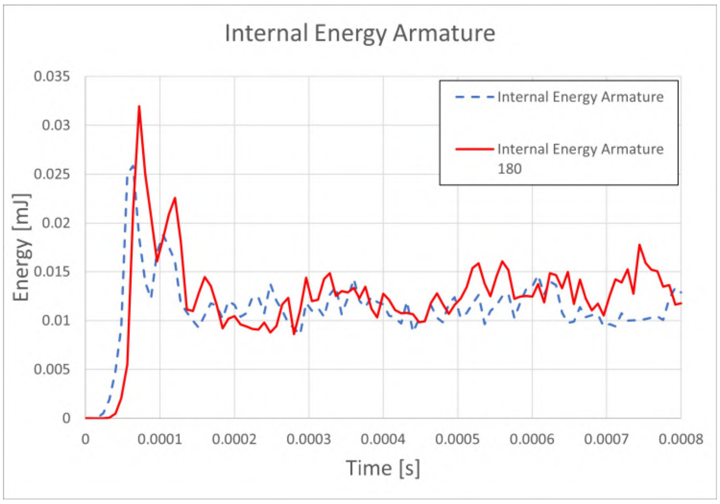

Figure 3.31: Internal energy of the armature

Internal energy of the membrane is higher in the orientation of 180 degrees (orientation B).

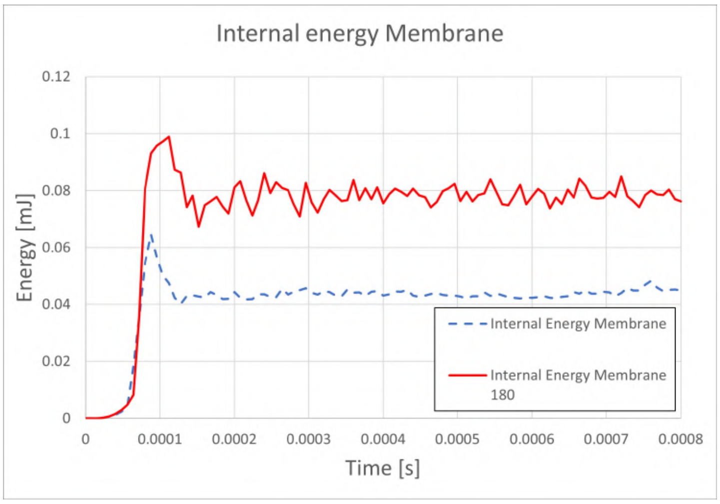

Figure 3.32: Internal energy of the membrane

The high internal energy of the membrane indicates there is more energy stored due to deformation. However in contrast to the higher internal energy, the local von Mises stresses in the membrane with the 180 degree flip are significantly lower. Both orientations reach values up to 600 [MPa], however orientations A has a higher concentration in the hinge than orientation B. The deformation in the hinges do have more consequences for the entire off-set.The higher internal energy but lower local stresses indicate that the deformations are more distributed over the entire membrane.

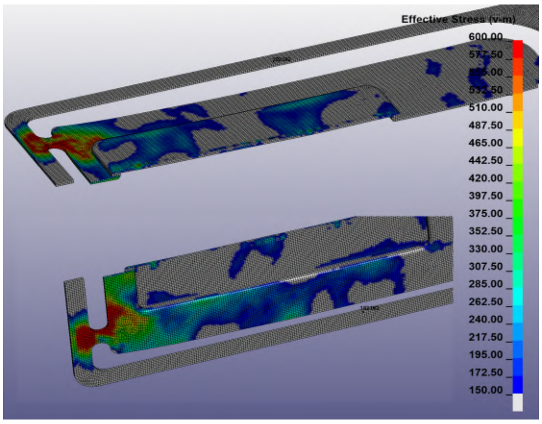

Figure 3.33: Reference von Mises stress membrane

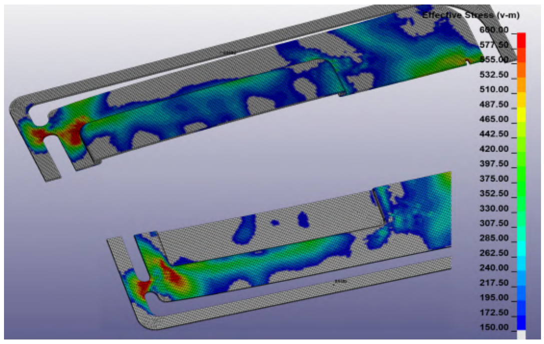

Figure 3.34: Von Mises stress membrane 180 degrees

3.4.5. Off-set After Shock

With the post processing software of LS-PrePost nodes can be selected separately. The region of interest for this experiment is around the hinges. To capture the deformation properly a nod will be selected close to the casing and a node just after the hinge. This distance is ± 500 μm (see figure 3.35), in this model that is the Z-direction. The next step is to plot the relative displacement in the Y direction. The Y direction is the axis on which the force is applied. Relative is important since the entire structure is moving. The point near the casing is the reference point for the point in the hinge. The simulation has a run-time of 2ms even though the plastic deformation ends after 0.5ms. An average value is taken over the time from 0.5-2 ms, this is done to get a good estimate of the deformation. This can be seen in figure 3.36. This value is 0.023328 millimetre or approx. 23 micrometer. Also this simulation is done without a cover so that the deformation can be compared with the experiment done in section 4.3.4.

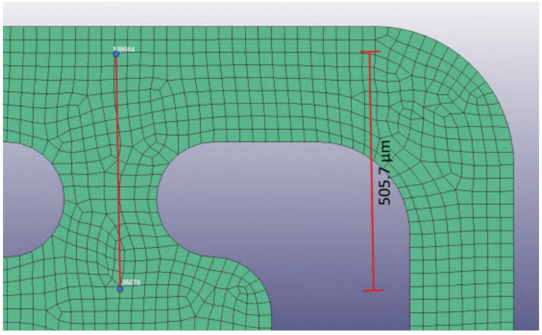

Figure 3.35: The selected nodes

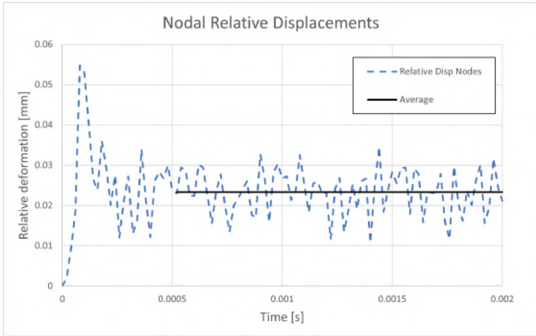

Figure 3.36: The relative displacement over time

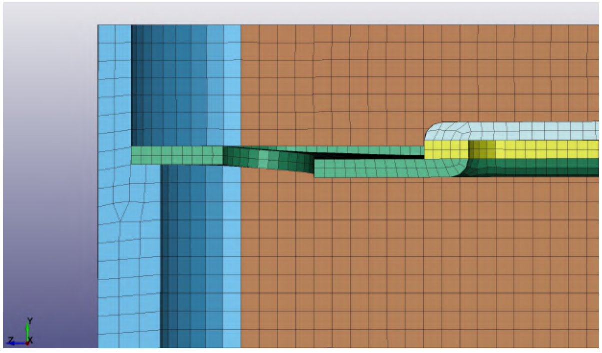

Figure 3.37: Side view from the off set on the hinge after 2ms

3.4.6. Shock Protection Armature

Comparison is made between a model without shock plates vs with shock plates with two different materials. The option 1 is made from nickel sulfamite and option 2 is made from nitrile rubber. The Internal Energy, von Mises stresses and Contact forces of the armature against the lower magnet are presented.

Energy

The internal energy in the membrane and armature present the amount of energy stored due to deformation. It can be seen that the shock plates have a little effect on the membrane. The results show that the armature displays a significant less internal energy. The material of the shock plates itself seem to have quite a large effect for the energy as well.

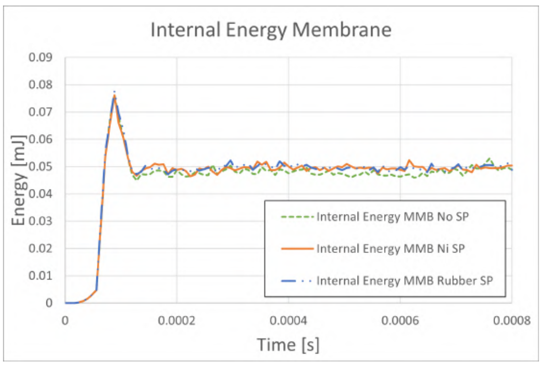

Figure 3.38: Internal Energy Membrane

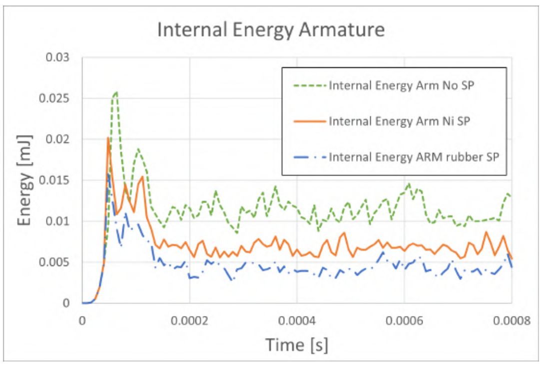

Figure 3.39: Internal Energy Armature

von Mises Stress

The simulation is a time dependent study, this means that the stress distribution changes over time. The von Mises stress displayed in the figure is at the time when all the stresses are highest. This done to pinpoint and highlight the critical regions of the structure. The stresses in the hinges become less severe with shock plates. The rubber shock plates even display less stress.

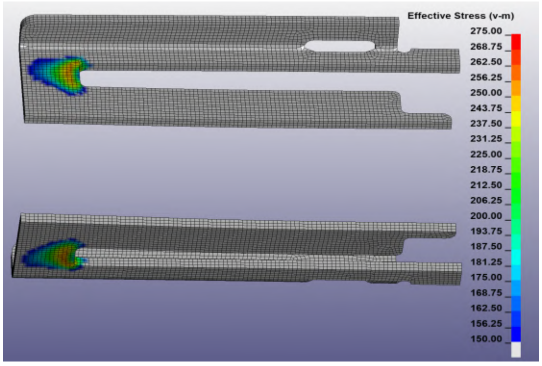

Figure 3.40: reference von Mises stress armature

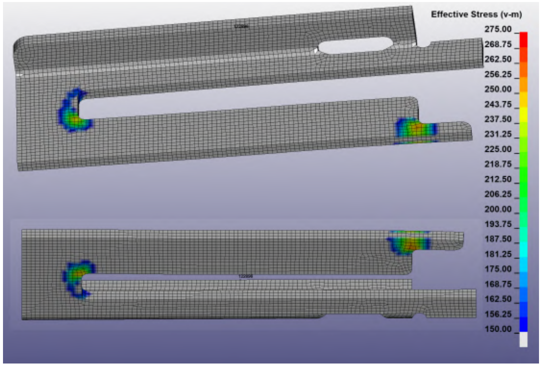

Figure 3.41: von Mises stress armature with Shock Plates

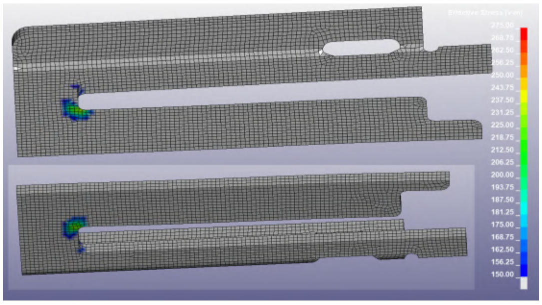

Figure 3.42: von Mises stress with rubber shock plates

The von Mises stress in the membrane is very high around the hinges. The sharp edges of the embossed are display also pretty high stresses. The influence of the shock plates is minimal in the membrane.

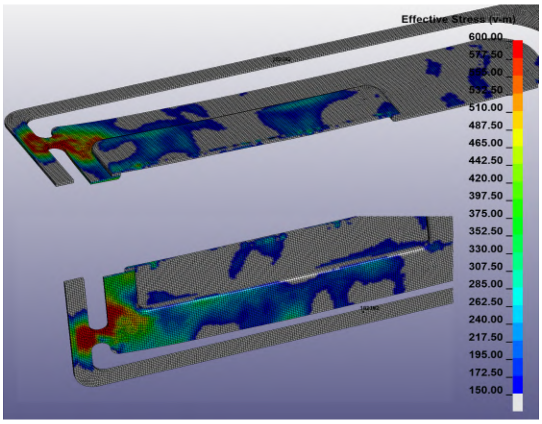

Figure 3.43: reference von Mises stress membrane

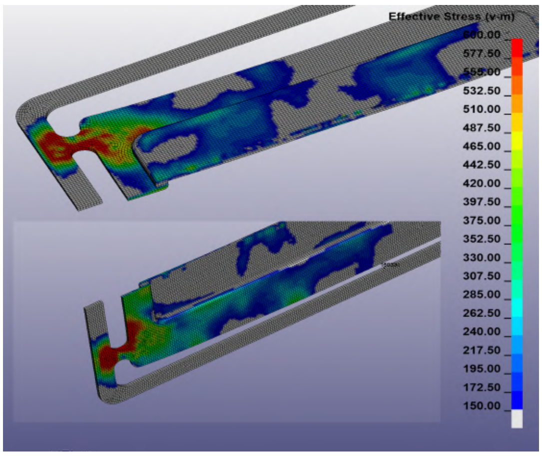

Figure 3.44: von Mises stress membrane with Shock Plates

Contact forces
The contact force in Newton between the armature and the lower magnet is a good indication of the effects of the shock plates. The Force measured is the resultant force, but is almost 100% dominated in the Y-direction. The impact of this force will likely not damage the magnet or the armature, but it does give a good indication if the shock protection dissipates any energy. The comparison of the severity of the impact between the different designs can also easily be derived from this result. Adding shock plates decreases the maximum contact force with almost 20%.

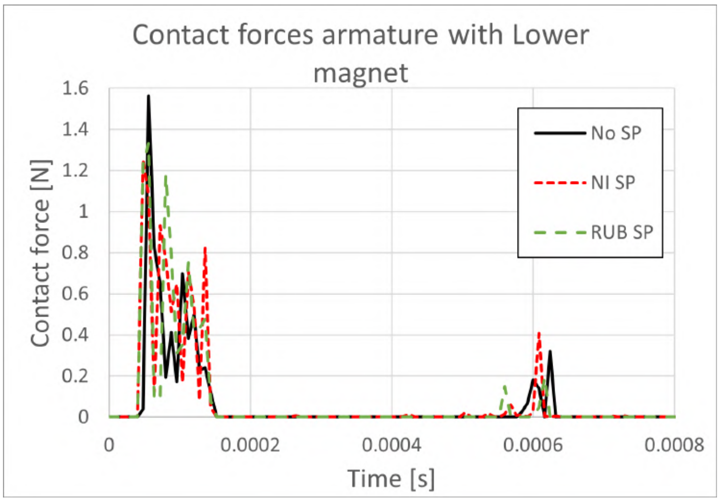

Figure 3.45: The contact force between the armature and the lower magnet

3.4.7. Changing the stiffness of the Membrane

The results of alternating the stiffness behaviour of the membrane on their shock response will be presented. Option 1 has no embossed are and thus a overall thickness of 50 micrometer. Option 2 has an increased thickness including the embossed area.

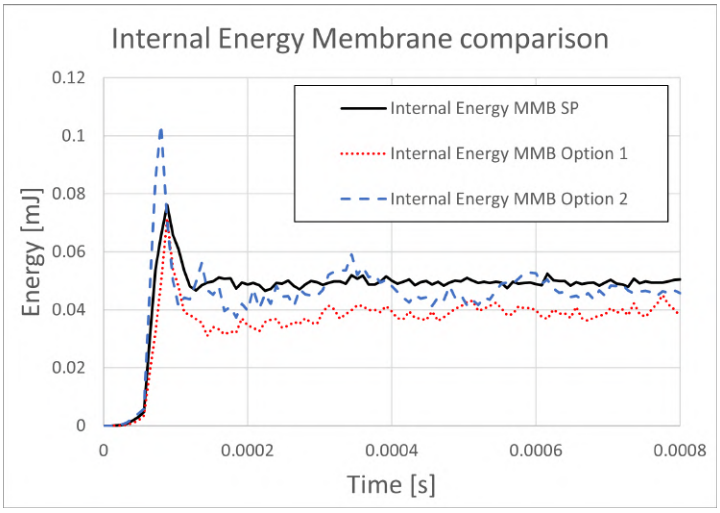

Figure 3.46: The internal energy in the different membranes with different stiffness

The results of the internal energy show that there is not much change (see figure 3.46). However a closer look at the plastic strain around the hinges indicate quite a difference (see figure 3.47). Option 1 has compared to the other two designs a lot more plastic strain. Option 2 has has less plastic strain at the embossed area as well as the hinge itself. This indicates that there is less severe plastic deformation in option 2.

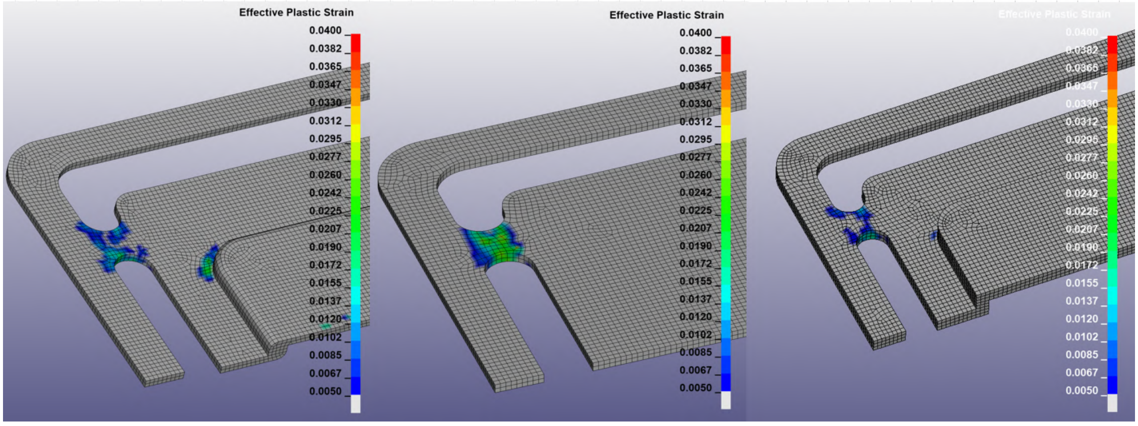

Figure 3.47: The plastic strain in the different membranes. Left = reference, middle = option 1, right = option 2

Fully Coupled Model

The dBSPL output FRF is plotted. The Ref Measurement are the results from the measurements performed before shocking. The COMSOL Ref is the simulation of the receiver as the receiver is without any modifications. The COMSOL ref model shows quite reasonable correspondence with the reference measurements. The COMSOL 100 micrometer MMB (MMB = Membrane) shows what happens to the output when the MMB thickness is increased by 50 micron. The COMSOL "No Embossment" MMB shows the Sound Output with a very compliant membrane.

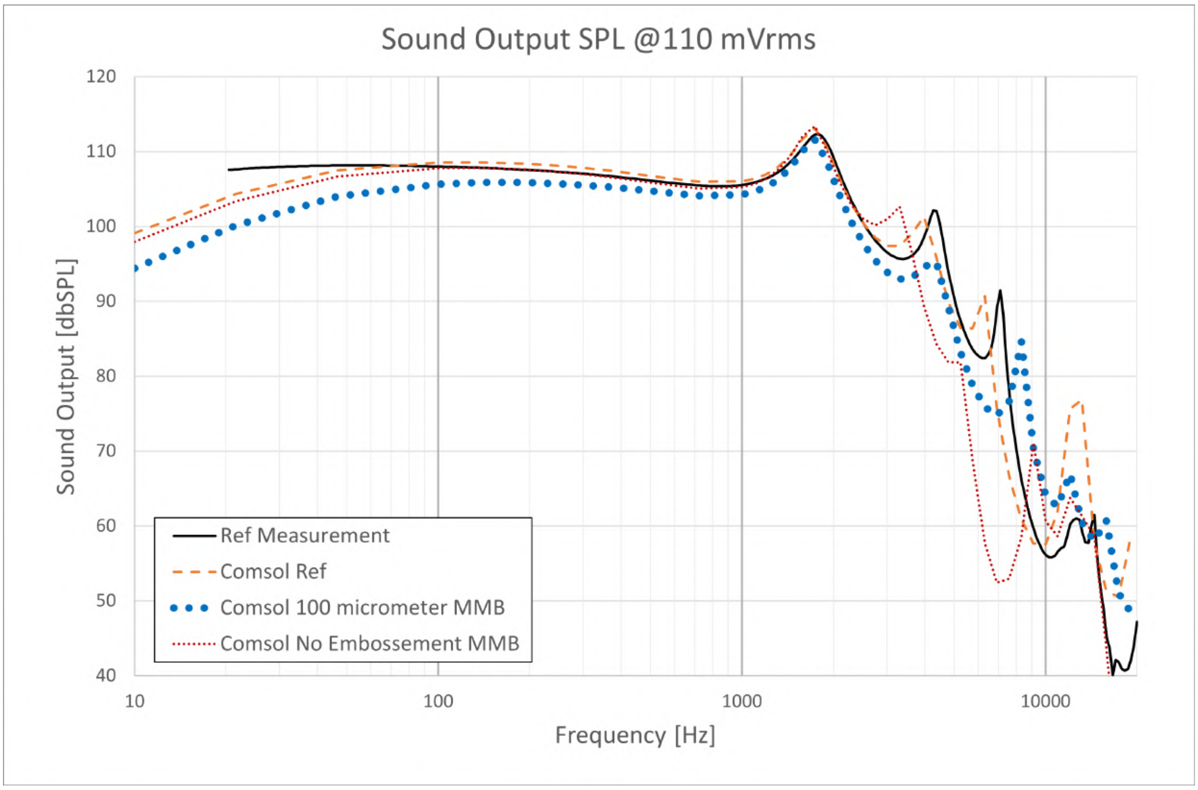

Figure 3.48: The dBSPL output FRF

4

Experimental set-ups, measurements and validation

This chapter contains the most important experiments and measurements. First the aspect of mechanical shock loading will be discussed followed by the methodology of different test set-ups. The different test set-ups include the measuring of the shock pulse, performance of the receiver before and after shock, mode shapes of the armature and the deformation of the membrane after shock with a 3D optical profiler.

4.1. Mechanical Shock

This section describes the classical and most common shock pulses, necessary theory and why they are used and which are relevant for this study. This will be followed by an methodology on how and what kind of shock pulse is found in this research.

The field of shock and vibration has a broad spectrum of intensity and can vary from earthquakes and small vibration to pyroshock and all magnitudes in between. Shock is defined as follows: "*Shock is defined as a vibratory excitation with a duration between once and twice the natural period of the excited mechanical system*"[27]. This sudden acceleration (or deceleration) can be excited by different sources such as impact or drop but also because of base accelerations such earthquakes or engine vibrations.

It is important to understand the physics of shock and drop when performing tests or modelling. There are different types of shock loading conditions to excite an object. This study focuses on mechanical shock. To narrow the scope, a field of interest is defined as the drop and shock environment of (micro) electronics. Testing of shock and drop has been of major importance in the design and testing of reliability of electronics [8]. The amplitude and duration can vary significantly and heavily determine the behaviour of a shock wave. The amplitude is usually defined by peak acceleration, which is given in either $[m/s^2]$ or $[g]$ which is 9,81 $[\frac{m}{s^2}]$. The duration is given in time [s]. The book of Lalanne [27] mentions two common mechanisms that lead to the degradation of a system. The first is exceeding a certain value threshold leading to permanent deformation or fracture. The second one is when shock repeated many times and fatigue will lead to failure. In this study the main interest will be on the first mechanism, exceeding a certain value threshold leading to permanent deformation or fracture.

4.1.1. Classical Shock pulses

In classical shock mechanics there are the principle idealised shock pulses. The principle idealised shock pulses are a single dominant pulse that is isolated. There is no focus on residual less severe shock waves, which often follows afterwards. A controlled impact collision between two rigid objects will generate such a pulse. The amplitude and duration of the pulse can be influenced by material and shape, often called the programmer of a shock impact test machine. If the desired pulse is a perfect symmetric half sine pulse, a high rebound and low damping of the material is required. If a saw-tooth like pulse is desired, low rebound and high damping is preferred [27]. The rebound and damping can be influenced by strategically choosing the materials. e.g. materials that have a good ability to absorb and dissipate energy will have a higher damping. By alternating the shape of the programmer one can also influence the shock wave pulse, Yang *et al.*[28] clearly demonstrates the differences between an conical lead programmer and a truncated conical programmer. Only the most important pulse is discussed, several other of the most used idealised pulses are briefly described and discussed in appendix D.

The half-sine pulse is probably the most applied in the field of drop and shock testing. If one would plot a graph of acceleration versus time, the curve represents a half period of a sine wave. This pulse waveform is often close to real measurements data and can be implemented in models with confidence.

The equation used for this half sine pulse is as follows:

$$\left.\begin{array}{ll} \ddot{x}(t) = \ddot{x}_m sin \frac{\pi}{\tau} t \quad for \quad 0 < t < \tau & \\ \ddot{x}(t) = 0 & elsewhere \end{array}\right\} \tag{4.1}$$

- τ = Duration/Time period
- $\ddot{x}$ = Acceleration
- $\ddot{x}_m$ = Amplitude of the acceleration (Peak Value)
- t = Time step

Idealised half sine shock pulses, see equation 4.1, are often used for drop tests performed on a drop table. The typical half sine pulse is suggested for drop tests by JEDEC (JESD22-B111) [29] [30] [7]. In most research where an idealised pulse is used, it is set as a boundary condition that acceleration is 0 for t $\geq \tau$. This would indicate an idealised situation with an idealised pulse, hence there are no residual oscillations after the pulse. The duration of the half-sine pulse influences the response, Shu *et al.* compares the pulse widths of the half-sine accelerations with the response as relative displacement [31]. He concludes that there is a critical value value for the frequency ratio to achieve the maximum displacement. The frequency ratio is the ratio of the characteristic frequency $\omega = \frac{\pi}{T}$ and the natural frequency.

$$\beta = \frac{\omega}{\omega_n} \tag{4.2}$$

- β = Ratio
- ωx = Characteristic frequency
- ω_n = Natural frequency

The peak value of the half sine is kept as constant, but the duration is set as a variable. The relative displacement increases sharply as the pulse width narrows (shorter duration). A validation of the acceleration pulse can be done with the use of accelerometers [9].

4.1.2. Drop and Shock instrumentation

Research of free fall or guided free fall drop tests have been studied as well. The test object have a direct impact with a hard surface. The waveform shock pulses of this direct impact will have a very sharp rise. Free fall allows the test object to rotate around all its axis and the orientation. The impact angle is not fixed and can differ every test. One of the aspects that will cause complications during these drop tests is the repeatability. Guided free fall tries to take care of this inconsistency and aims to improve the quality of replicating the experiment. This principle work pretty well for a larger scale object, however it seems to be very difficult to keep the consistency of the drop angle at a high level while testing balanced armature receivers.

In the paper of Tempelman *et al.* the test set-up is aimed to guide the drop object until it hits the striking surface [32]. The design of their drop tower allows for accurate control over the impact angle for product drop test. At Sonion Nederland R&D an advanced guided free fall machine is available (see Fig 4.1). The Heina DT2000 is able to use a small vacuum tube, or for larger objects a clamping feature, to maintain the position of the test object until a few centimetres above ground and then release the object.

Figure 4.1: Guided Free fall (Heina DT2000) available at the research facility of Sonion Nederland B.V.

Studies from Sonion in the past with high speeds cameras have shown that the angle of impact of the balanced armature receiver is slightly different every time. Using very large sets of data might give some insight on the level of failure, however due to the scope and aim of this study this will not be investigated.

4.2. Experiments and Measurements

This section discusses the methodology of measuring the shock wave with the pendulum tester. Measurement of the performance of the balanced armature receiver before and after applying shock loading conditions. Model analysis experiments are set-up to give insight in the structure and validate FEM analysis. Finally experiments are set up to correspond the final off-set to relate to the explicit FEM analysis performed in Ansys LS-Dyna.

4.2.1. Methodology for determining the shock pulse

In order to determine the correct shock pulse there are the following variables that need to be measured; the magnitude (peak acceleration[g]), duration [s] and the waveform itself. The impulse, a force as a function of time, can be seen as impact. According to the book of Hibbeler [33] "*Impact occurs when two bodies collide with each other during a very short period of time, causing relatively large (impulsive) forces to be exerted between bodies.*". A pulse that is applied in a certain axis, will have a negative relative displacement in the structure of the test object [11]. Displacement is mostly measured in the same axis the acceleration pulse. The mechanics of Impact have a period of deformation and a period of restitution. An illustration of the shock generated by the tester can be seen in fig 4.2.

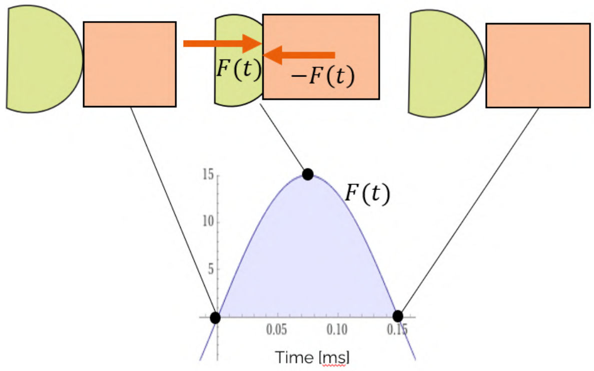

Figure 4.2: The illustration shows how the force will be a function of time

A test set-up for determining shock can be seen in the calibration set-up (see figure 4.3). By raising the pendulum the magnitude will increase, the duration however will be less prone to the position of the pendulum. The duration of the shock pulse is mostly influenced by the material and geometry, which both do not change over the time of the experiments. Therefore it is expected that the change in duration will not show any significant changes. The expectation is that the geometry and material of the test set-up will measure an acceleration shock pulse that approaches a half sine waveform.

The process of calibrating the shock tester is combined with the opportunity to test the waveform of the exact shock pulse. An overview of the test set-up can be seen in figure 4.3. A low impedance piezoelectric compression accelerometer, will be screwed into the end of the pendulum. The piezoelectric accelerometer is the Low impedance piezoelectric compression accelerometer form Bruel and Kjaer type 8339. The piezoelectric elements produce a charge proportional to the force. The accelerometer sends the electrical signal is sent to the amplifier. The amplifier is a measuring amplifier type 2525 from Bruel and Kjaer. The accelerometer is connected with a low noise cable to the amplifier as can be seen in figure 4.3. The amplifier is connected to the Rhode and Schwarz digital oscilloscope. The oscilloscope will display the measured signal, which still has the units of micro voltage over time. Setting up the amplifier one should provide the correct sensitivity and gain. This measured signal can than be converted into acceleration [g] over time. This information can be used to compare with classical half sine or other classical pulse shapes. This then can be used as an input in the finite element model.

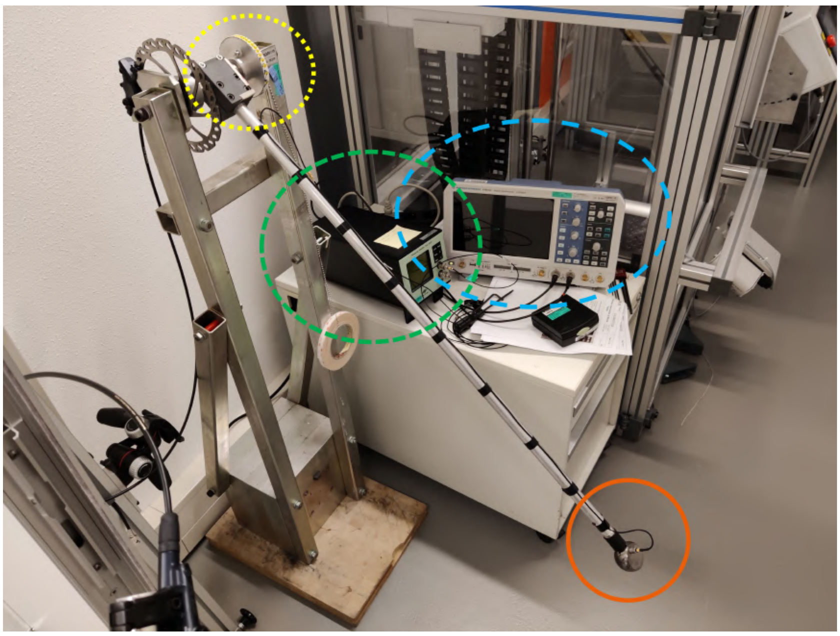

- Small dashed line (yellow) - Control panel to set the required amount of shock [g]
- Dashed line (green) - Measuring Amplifier type 2525 (Bruel and Kjaer)
- Large dashed line (blue) - Rohde and Schwarz Oscilloscope - 2.5GSa/s
- Solid line (orange) - Low impedance piezoelectric compression Accelerometer Bruel and Kjaer type 8339

Figure 4.3: Calibration Set-Up

The first calibration measurement starts with a 1000 [g], once this is set correctly the height will be increased with a 1000 [g] each time (see fig 4.3 and fig 4.4). This step will be repeated until a maximum has been reached of 19k [g], the accuracy of the accelerometer is not guaranteed with higher acceleration plus the set-up can barely reach higher accelerations than this. Each measurement will be done twice for better quality. The admissible difference of the measured average is ±3%. When the deviation is not within this limit, the launch values must be redefined. Once the pendulum has been brought the desired launch value, the oscilloscope must be ready to capture the shock. After the shock the second bounce back must be prevented by braking again and thus bringing the set-up back in equilibrium.

Figure 4.4: The Control Panel to set the required amount of shock

4.2.2. Material Models

Depending on the situation material properties are generally known in material databases, provided by the supplier or must be defined through material testing. The materials of balanced armature receivers are treated to meet specific requirements and the properties are therefor unlikely to be known specifically unless tested within own R&D of given by the supplier. One of the materials that is not used in the product itself but must be taken into account is the double sided tape with which the balanced armature receivers are mounted to the pendulum shock machine. Contact with the manufacturer resulted in the desired material properties.

The most critical components of the balanced armature receiver for mechanical testing under drop and shock loading conditions are the membrane, armature, drive pin and the casing. The material properties of the Nickel Iron alloys are tested by an external company. The stress and strain curves of the NiFe 50/50 and the NiFe 80/20 are provided in the appendix B. The properties of the other materials are found in the Granta database. Granta is a company that provides an online database with a wide variety of materials and their given properties.

4.2.3. Sensors

Accelerometers are often applied to obtain measurement data about mechanical shock or vibration. For high acceleration tests low impedance piezoelectric compression accelerometers are advised. The sensors are attached to either the object itself or the base frame [16]. In this research a Low impedance piezoelectric compression Accelerometer Bruel and Kjaer type 8339 is used to measure the pendulum impact. The waveform input shock pulse can be accurately measured. In this study the object to test, a balanced armature receiver, is too small to directly fit the accelerometer. However the accelerometer can be fitted into the pendulum head. The Sensor is screwed in the pendulum head with an optimal mounting torque of 1.8 [Nm]. This measurement provides validation and information about the acceleration input for the FE model.

For the nodal analysis the sensors of the laser vibrometer, the polytec PSV 400, will measure the displacement, velocity or acceleration on a predetermined coordinate(s) on the armature. A fixture will be mounted on a shaker which will be driven over a range of frequencies. The laser head of the machine allows to measure the vibration, either velocity or displacement. The peaks of the frequency response indicate eigenfrequencies. By creating a laser grid the software has the capability to measure and model mode shapes that might help with visual analysis and better understanding the mode shape.

4.2.4. Balanced armature receiver output

Testing the performance of the balanced armature receiver before and after the drop and/or shock is a good indication of any failure mechanisms. One of the key performance indicators of a balanced armature receiver is the frequency response of the sound pressure output. In order to capture the failure process properly it must be tested how the performance is decreasing or whether the receivers stops working at all. The performance can be measured in different ways, the sound pressure output in [dBSPL], the Total Harmonic Distortion (THD) in [%] and deformation in [μm].

In order to measure this output, the Sound Pressure Level (SPL) can be measured by connecting the receiver to an voltage source. This source drives the receiver and can be controlled to excite the balanced armature receiver over a specified range of frequencies. The range will be from 20Hz to 20kHz, since this is the region of interest because that is what the human ear is capable to hear.

The balanced armature receiver is placed in a jig that fits a particular type of receiver, in this study the 31A007G balanced armature receiver from Sonion will be used. The balanced armature receiver is than driven with a voltage source that can be controlled and programmed via the Audio Precision APX500. The balanced armature receiver will be driven at nominal drive which is according to the data sheet 110mV RMS. The spout of the receiver is coupled to a tube, this can be a long or short tube. The long tube ($\pm 30mm$) represents the cable from a hearing aid to the ear used in Behind The Ear receiver models (BTE). The short tube ($\pm 3mm$) is used to replicate the In The Ear receiver (ITE). In this thesis the short tube will be used since this creates less acoustical mode shapes (eigenfrequencies). Less unwanted eigenfrequencies in the result show more clearly the effect of drop and shock. The tube is than coupled to a ear simulator (also called Coupler). This experiment the 2 CC coupler from Bruel and Kjaer will be used. The ear simulator is coupled to a microphone (which represents the eardrum). The microphone will measure an output, for example in millivolt per micro pascal, this is than again converted to dBSPL.

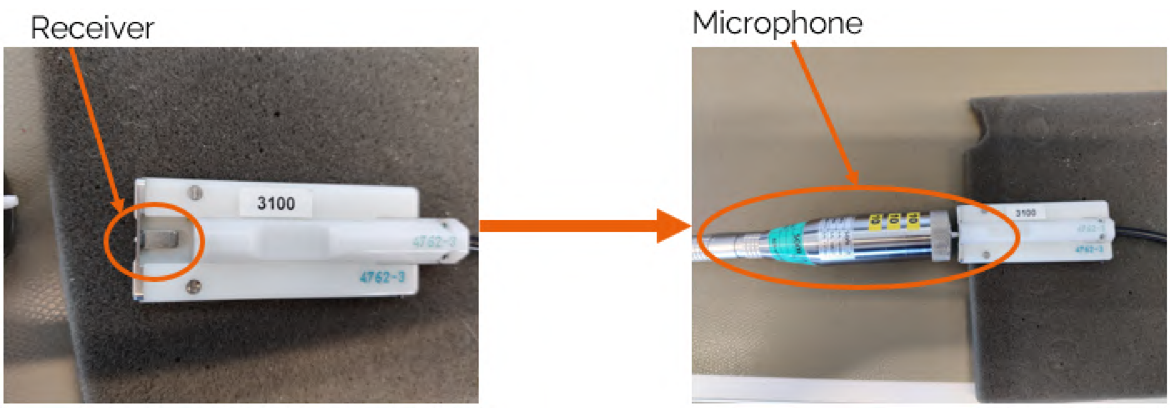

Figure 4.5: A set-up of the receiver in the customised jig and the connection to the microphone

Equipment for measuring the performance of a 31A007G balanced armature receiver

- 31A007G balanced armature receiver from Sonion
- Jig for the balanced armature receiver
- Measuring Amplifier (Bruel and Kjaer)
- Audio Precision APX500
- Bruel and Kjaer 2cc coupler
- Bruel and Kjaer 1" microphone type 4144

4.2.5. Total Harmonic Distortion

In the paper of Jeremy Agnew [34] Total Harmonic Distortion (THD) in hearing aids is described as undesired frequencies that are harmonics of an input frequency that are created in the output. The original or first harmonic is often called the fundamental harmonic. The basic formula for THD is as follows:

$$THD = \frac{(Output - Fundamental)}{(output)} \tag{4.3}$$

or

$$THD(\%) = 100\sqrt{\frac{f_2^2 + f_3^2 + f_4^2 + ...}{f_1^2 + f_2^2 + f_3^2 + f_4^2 ...}} \tag{4.4}$$

In the hearing health industry the threshold is usually defined by the by the paper of Dillion and Macrae [35]. It is stated that for hearing aids the distortion is preferably less than 5% and should not exceed 10%. Other studies have shown that the human ear can be sensitive to a THD as low as 0.1% [36] . The threshold of less than 5% is mentioned in the paper of Jeremy Agnew [34] which is from 1998 but the paper of Zoe Yee Ting shows that in more recent studies (2015) the standard set by Dillion and Macrae is still used by the hearing health industry [37]. This standard is also used often at Sonion Nederland B.V. and therefor these values will be used as well in this thesis to partly analyse the performance after drop and shock. The set-up is effectively the same as for measuring the SPL. Additionally to the Total Harmonic Distortion, it is helpful to focus at the 2^{nd} Harmonic. Even harmonics indicate asymmetrical distortion, which mean a off-set in the membrane or a asymmetrical magnetic picture. In other words if the receiver is unbalanced the receiver will create dominantly second order harmonics.

After a frequency sweep at a constant voltage, it helps to perform another sweep. This time the frequency is held as a constant and the voltage is swept. The constant frequency can be the half peak value of the eigenfrequency.

4.2.6. Failure Analysis Challenges

The post-processing actions such as analysis of high stresses, strains, deformation and deflection are the most important to draw conclusions about the failure mechanisms. When using the post processing methods of FEM it is relatively easy. The difficulty for a FE model is that it will generate huge amounts of data, being critically selective is essential to process this. The methods to measure with real experiments on the other hand are difficult to apply because of the size and closed casing of the balanced armature receiver. Stress and strain sensors are mostly not capable to measure within this order of magnitude without affecting the results. Also High Speeds camera's have difficulties with these high acceleration plus the fact that the region of interest is inside a closed casing. It is possible to validate components separately, the armature, one of the most important components will be tested via modal analysis. To gain more confidence in the accuracy of the FE model, a shock test with an open cover can be performed and measure the deformation of the membrane before and after shock excitation. More info can be found in section 4.2.8.

4.2.7. Modal Analysis

The eigenmodes provide useful information about the structure before even shocking the balanced armature receiver. The modal analysis will provide the eigenfrequencies (or natural frequencies) which are the frequencies at which the structure is prone to vibration. The corresponding mode shape indicates on how the structure will vibrate.

In order to determine/validate the mode shapes of the armature a fixture device is designed and made with the help of the by the DSS department (Development Support Services) of Sonion. Only the armatures are clamped in this structure, so there is only the mechanical response (see fig 4.6) and no influence of any acoustical stiffness. The way the armature is fixed is important since it heavily affect the response. Thus the fixture clamps the armature similar to the way it is fixed in the balanced armature receiver itself.

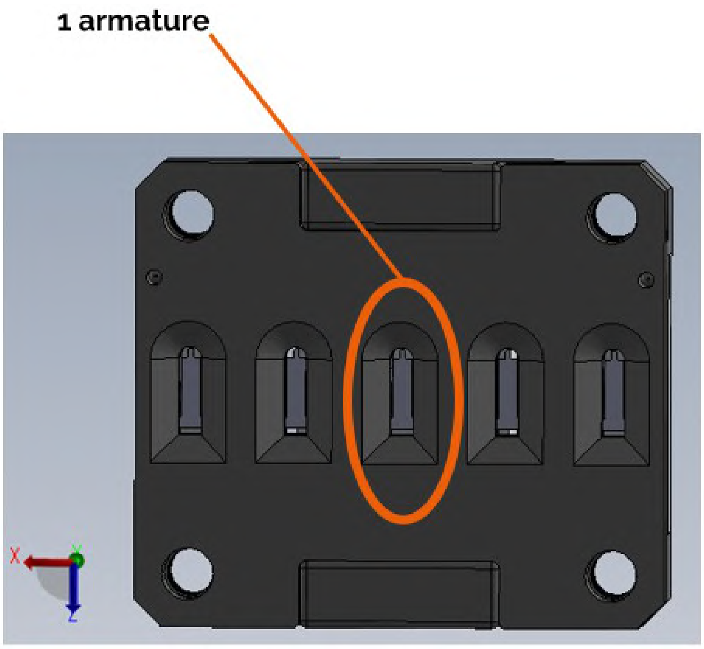

Figure 4.6: The fixture device which is able to fix 5 armatures at the same time

The set-up of the experiment is drawn schematically in fig 4.7. The solid orange lines represent BNC cables. The fixture that is mounted on the shaker is driven by a signal that originates from the corresponding PSV 400 Junction box, but is amplified by the amplifier. The output of the amplifier is also measured to determine the phase.

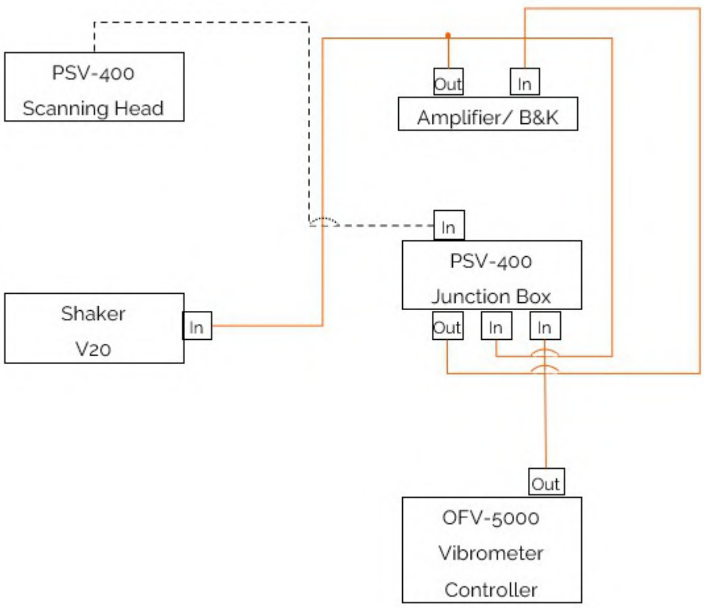

Figure 4.7: Schematic set-up of the experiment

The fixture is screwed into the V20 shaker, which is positioned on a hydraulic table to cancel external vibrations. The shaker is driven by the PSV 400 via an amplifier which sweeps over a range of frequencies. The setting for this is pseudo random. With the polytec scanning head a single point or a laser grid can be made on top of the membrane. Once the laser is calibrated and set to the selected point or grid, the velocity or displacement can be measured. It is important to do this on the membrane but also on the fixture itself. This way we can afterwards eliminate the FRF of the fixture and only end up with the FRF of the armature itself. If the armature is isolated it can be compared with the COMSOL model made previously. The single point will be used to determine the frequency response. The peaks of this response indicate the eigenfrequencies. Because of the laser grid of the polytec machine it is also possible to measure also the mode shapes. The mode shapes and eigenfrequencies can be compared with the model made in the COMSOL eigenfrequency study. This will give validation and more confidence in the models used.

4.2.8. Deformation of the membrane

From the results of the simulations it is likely that the membrane will undergo plastic deformation after being exposed to high accelerations. With the post processing software the FE model is relatively easy to analyse, spot where and how severe this deformation is, hence the value of Finite Element Analysis. For validation and experimental measurements this is more difficult on this scale. An alternative method that must give the confidence that the FE model is correct must be found. The balanced armature receiver can be assembled without a cover and a foil, from now on called an open motor receiver. It is important to have the samples assembled without cover and foil instead of removing these components from the complete balanced armature receiver. Removing these components heavily damages the structure, even while being careful. With special thanks to the production of Sonion in Vietnam the assembly was possible without foil and cover. Removal without damage of the cover and foil can also easily be done in the geometry of the FE model. Without a cover it is now possible to use scanning technology from above. This is done before and after shocking the balanced armature receiver with the shock test machine (see section 4.2.1). Ten samples are shocked with the highest amount of acceleration possible on the tester, 19k [g]. After this shock test the samples will be measured again. The measurement points will be around the hinges since this is where the most plastic deformation takes place. The finite element model is an ideal situation, thus symmetry conditions can be used. Thus only one hinge can be used. The real samples always have some sort of off-set or asymmetry. Ten samples will have 20 hinges.

Figure 4.8: 3100 balanced armature receiver with open motor

The equipment that will be used to perform a three dimensional scan, is the Sensofar S Neox a 3D optical profiler, which is state of the art equipment of metrology. The International Bureau of Weights and Measures (BIPM, 2004) defines Metrology as *"the science of measurement, embracing both experimental and theoretical determinations at any level of uncertainty in any field of science and technology,"* . The Sensofar S Neox uses confocal microscopy technology to obtain accurate results. The depth profile is measured along a line across the membrane. Post processing two point are defined with approx. 500 μm distance. By comparing the distance in the Z-direction (the depth) before and after shock the relative off-set in the membrane hinges can be measured.

4.3. Experimental Results

In this section results are presented from the different experiments. The first results present the results from measuring the pulse acceleration. Secondly the results of measuring the performance before and after certain shock levels are determined. This includes the frequency sweep measuring the pressure output as well as the distortion. The results of the nodal analysis are presented. Finally the results from the Sensofar Scan of the deformation of the membrane are presented.

4.3.1. Shock pulse determination with a calibration measurement

The graphs (figure 4.9 and 4.10) present the acceleration [g] on the vertical axis and the time [s] on the horizontal axis. A sweep is performed starting with 1000 g until 19000 g. The presented signals in figure 4.9 and 4.10 are filtered of the eigenfrequency of the accelerometer itself. An example of the unfiltered signal can be found in figure D.1 in appendix D.

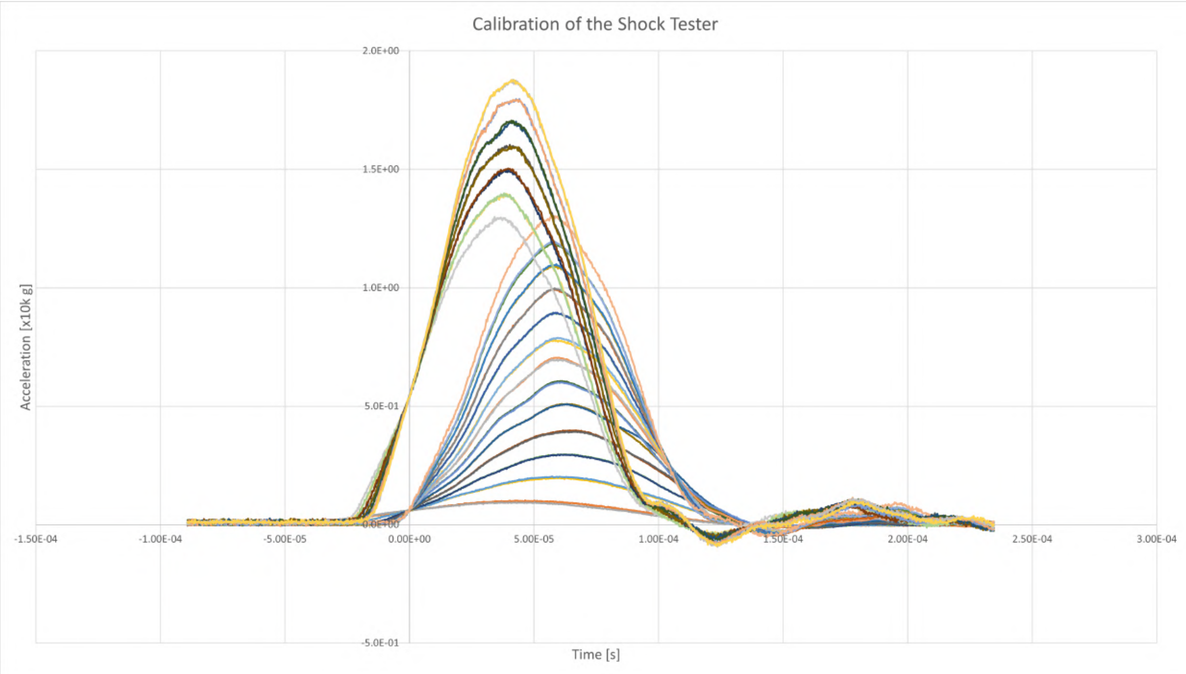

Figure 4.9: Calibration of the different shock levels

Figure 4.9 shows all the results of the calibration measurement. Every level of shock, starting with 1k g up until 19k [g], has been measured and the shock tester calibrated. The graph shows a slight shift in time, but not much in the duration. All the measurements have a duration of approximately 0.15ms.

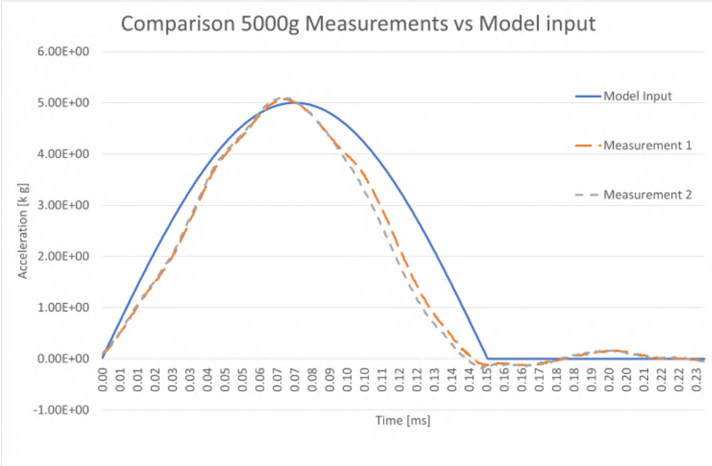

Figure 4.10: The shock pulse of 5k g vs an idealised half sine of 5k g

The idealised pulse (The half sine) and the measurement data have a small deviation when comparing them, but to reduce complexity for the model and increase flexibility a half sine shock wave will be used.

4.3.2. Performance and Shock level determination

To determine how severe the shock must be in order to properly analyse the failure mechanisms, one must understand and compare the performance of the receiver before and after certain shock levels. A clear rise in THD can be seen, specially after 14k [g].

Frequency sweep

The dBSPL output of the receiver and THD are measured over a frequency sweep with a constant voltage of 110 mV. The frequency response is presented in fig 4.11. This measurement is performed often within Sonion to test asses the quality of the receiver.

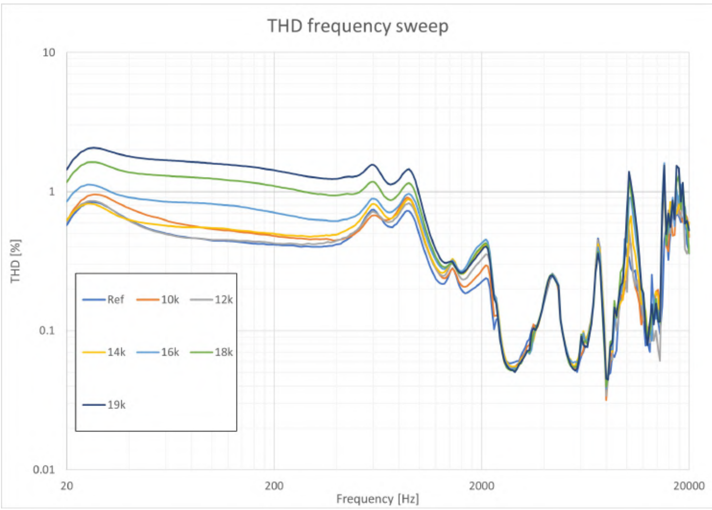

Figure 4.11: Frequency Sweep at 100mV

Voltage Sweep at half peak frequency
The voltage is swept while keeping the frequency at a half peak value.

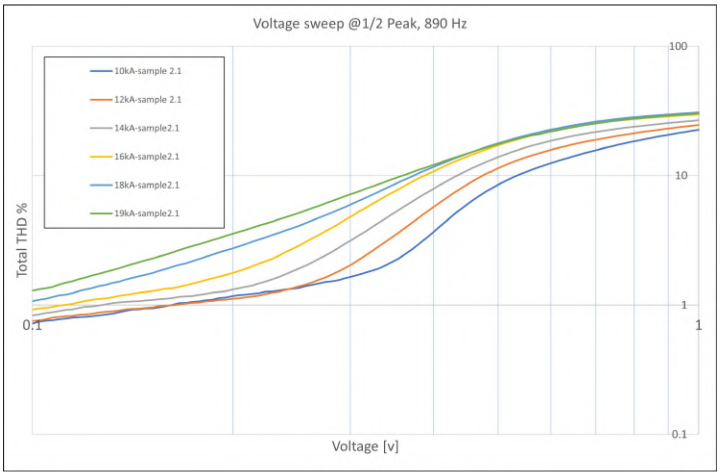

Figure 4.12: Voltage Sweep

4.3.3. Modal analysis

The FRF of the displacement of five armatures were measured and plotted against the Simulation in COMSOL. The armatures in the fixture were measured and the fixture itself (see fig 4.6). With the phase shift taken into account the armature could be isolated. This is now comparable to the COMSOL simulations (see fig 4.14).

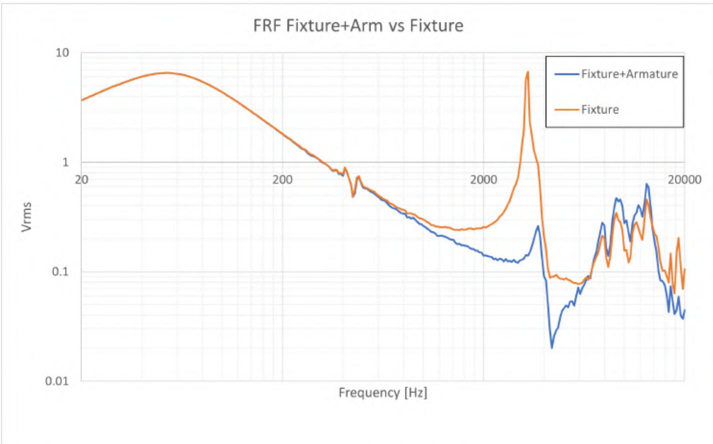

Figure 4.13: FRF of the measured samples in the fixture and the fixture only

Up and until the first resonance peak there is a good correspondence of the measurement and the simulation see fig 4.14. The higher frequencies have less correspondence, however these higher frequencies are of less interest. The higher frequencies contain quite some noise.

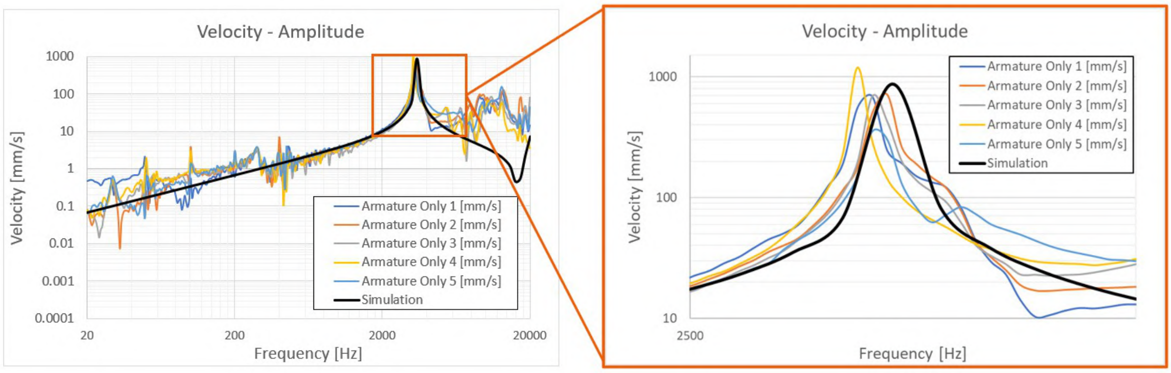

Figure 4.14: FRF of the measured samples and the simulation

4.3.4. Membrane deformation

A line is post processed on the membrane to project the curvature and deformation of the membrane. Two point are chosen on the hinge of the membrane. One close to the casing and one ± 500 μm distance. Since every sample is slightly different it is important to take the difference of the same sample before and after shock to properly capture the deformation. In the figures 4.15 and 4.16 the scan can be seen. This experiment corresponds to the FE model in section 3.4.5.

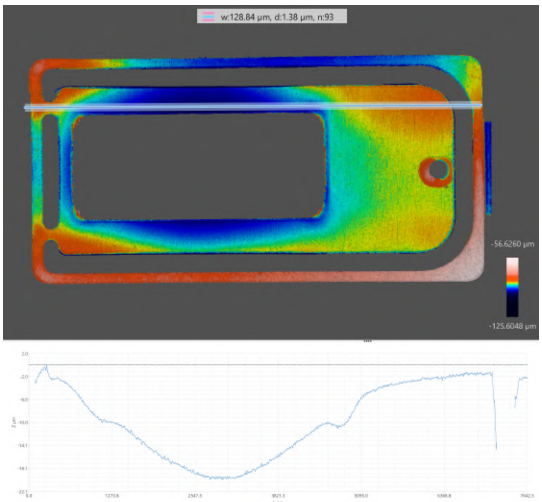

Figure 4.15: The entire membrane scanned

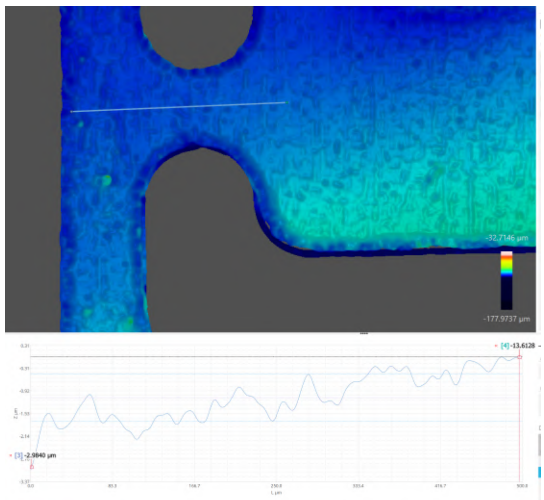

Figure 4.16: Zoomed in on the hinge

The results of the off-sets are presented in figure4.17 and 4.18. In rare case the off-set before shock was positive. The results are presented per hinge, so 1 and 2 belong to one sample. The delta is the difference found after shock minus the difference before shock per sample. The black line presents the simulation which resulted in a average of approximately 23 μm.

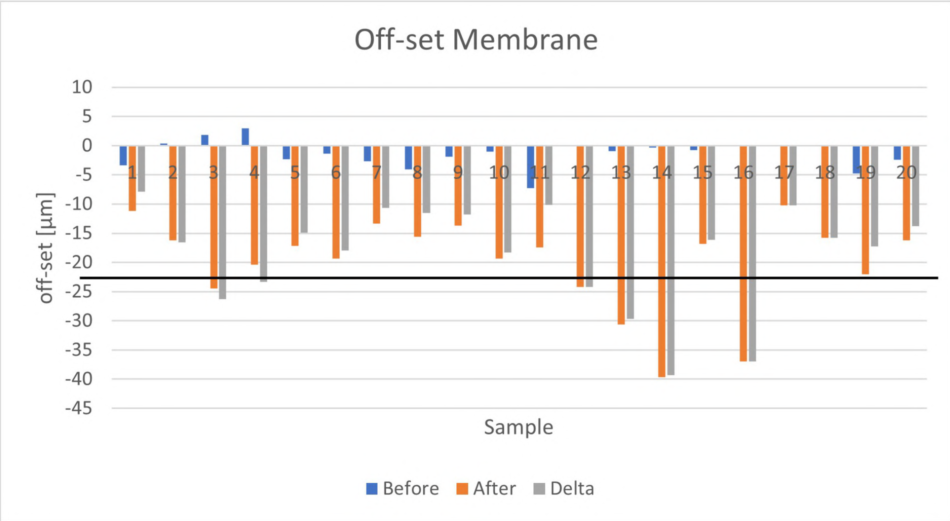

Figure 4.17: The off-set, before, after and difference per sample

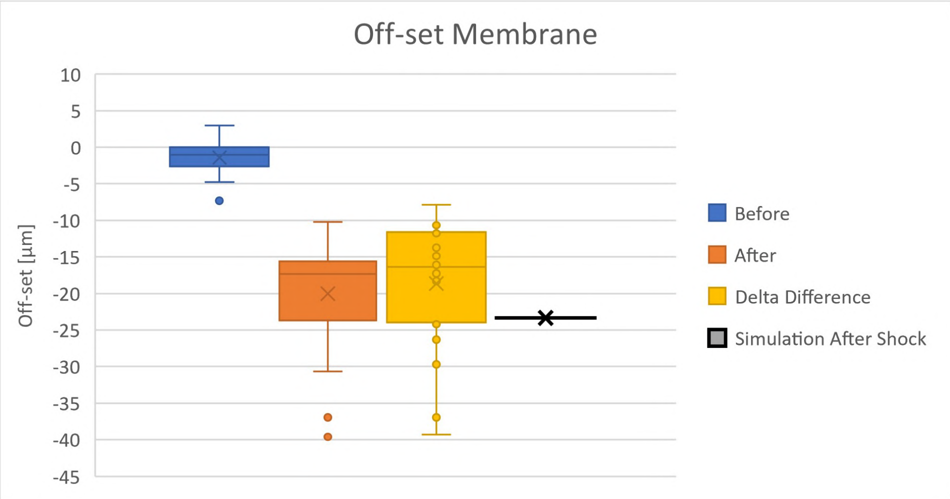

Figure 4.18: A box plot of the results

5
Discussion

In this section the results from the modelling and simulation part as well as the experimental part are discussed. The results and methods from both sections will be linked. First the different aspects of the shock pulse investigation are discussed. Then the critical regions of the balanced armature receiver are discussed and how this relates to virtual prototyping. Finally the experiments and measurements and how they relate to the model are discussed.

Shock pulse

The measured shock pulse closely reassembles an half sine, with a duration slightly shorter than expected. In literature comparable studies mostly accounted for 0.5ms duration whereas 0.15ms is measured in this set-up. This is valuable information for the input of the finite element models. Via applying a force, the correct acceleration can be used as input for the FE models. A combination of the input G and large mass method gives full control of the shock excitation while keeping the simulation accurate and reduced run time. By idealising the pulse into a half sine, it allows for easy adaptations to study the effects of changing amplitude or duration. For the FE model it is assumed that after the half sine there is no acceleration input anymore, however in the measurement it can be seen that there are some residual oscillations in the shock wave. The residual accelerations are magnitudes lower than the peak amplitude. Simulations of low accelerations, like these residual oscillations, have shown that they do not cause any permanent deformation and thus makes it acceptable to assume no residual oscillations after shock. The addition of the double sided tape does not impact the results that much but implementing it does make the model more realistic. The study on the orientation, where the receiver is flipped 180 degrees, is necessary to perform. Balanced armature receivers can have different shaped armatures which might be more sensitive to the orientation which the load is applied. For example for this product the orientation has little impact on the armature, however an U-shaped armature could experience a more orientated response.

Critical regions and virtual prototyping

Reviewing the results of the multiple experiments that have been performed, there are some interesting insights about the critical regions. As expected the hinges in the armature display a lot of high stresses. These stresses seem to reduce as soon as shock protection is added, but new high stresses arise in the connection area of the drive pin. The high stresses in the hinges do approach and sometimes exceed the von Mises yield criteria. This means that there will be plastic deformation what will effect the balanced position of the armature or create an off-set in the membrane. The robustness of this armature is improved by adding shock protection for the armature. The material of the shock plate influences the response under shock loading. By modelling shock plates made from Nitrile rubber, the armature hinges result in less concentrated stresses. With shock plates the stress concentration around the drive pin increases, however this will be less severe for the performance, since the balanced position of the armature is not affected by this deformation. The internal energy stabilises at a much lower lever when the shock plates are added. This decrease indicates less deformation in the armature, since internal energy is defined as energy stored due to deformation. Also it can be observed that the contact force between armature and magnets are improved after implementing the shock plates. The rubber nitrile shock plates show a similar first impact, the second impact is significantly lower with the rubber. This indicates that the rubber has slightly better dissipation of the energy compared to the nickel sulfamate.

The membrane has higher von Mises stresses and more deformation than expected. The hinges are vulnerable to the high accelerations. This is partly due to the thickness and stiffness of the membrane. The embossed area, which contributes to the entire stiffness, shows concentrations of high stresses as well. These high stresses are around sharp edges which is makes sense. The two different options of the virtual prototypes predict nicely the effect of the changes of the stiffness. option one is an overall more compliant membrane, which results in larger deformations. These larger movements are restricted by the fixation near the edge thus creating high stresses at those locations. The thicker membrane has approx the same amount of internal energy, but the deformation is much lower. This means that the final damage will be less severe. But increasing the thickness which such an amount comes at a cost.

This can be seen in the Fully Coupled Model from COMSOL. A thicker membrane results in lower output in the lower frequencies. The first peak is barely effected with both options, this is because the first eigenfrequency is dominated by the eigenfrequency of the armature, which is kept the same. The loss of output with the thicker membrane can also be found in the second peak, which is now much more damped. The membrane without embossed area has the same peak value as the reference however it is shifted to the lower frequencies. For the thicker membrane the third peak is also shifted to the higher frequencies and has a much lower peak value. This is even more severe for option without embossed area. To wrap up, the increasing of the thickness gives a stiffer and more robust receiver under shock loading however this comes at a cost in the FRF output of the receiver.

Validation

Because of the fixture that has been made, it was possible to validate the armature's frequency response directly. The most interesting eigenfrequency of the armature had a very good correlation with the model. The shaker tool itself had quite the influence on the response, but by measuring both it could be calculated to isolate the armature. This validation of the armature helped with gaining confidence for the model, this includes the material models, set-up and geometry.

For validation of the membrane deformation after shock it is possible to link the results with the experiments without a cover. The reference measurements of the open receivers before shock are a good example that every sample is different and no are perfect. Whereas in the FE model everything is ideal. But by looking at the measurement before and after a trend can be found in the deformation. Precaution is needed since the simulation is a dynamic simulation which is still moving at the end of the simulation, thus a dynamic situation is compared to a static one. However the the plastic deformation ends at half the simulation, also section 3.4.5 shows a plateau of the relative displacement. All together this would give confidence in the model to trust it when modelling with cover.

The fully coupled multiphysics model made with COMSOL helped with a better insight in the behaviour of the balanced armature receiver. The reference model could be improved in the future to better correspond with the measurements. However for the purpose of this study the model suffice as the correspondence is already good enough to give insight on the response of changing the membrane stiffness.

6
Conclusion and Future Work

6.1. Conclusion

This study focused on different aspects of the failure mechanisms of balanced armature receivers under drop and shock loading conditions. First of all it was important to have a proper controlled shock environment and translate this into the finite element models. The measurement set-up with the accelerometer and the pendulum tester made it possible to find information on how the shock pulse forms over time in this set-up. With a combination of modelling techniques this waveform could be correctly implemented in the FE models. The techniques allow for accuracy while reducing computational time and power. Knowledge has been gained and documented on how to prepare, set-up and check different types of models in Finite Element Analysis. This includes the models for impact shock analysis, modal analysis and multiphysic analysis. One of the major challenges was validation through direct measurements for the balanced armature receiver. Alternative methods were found to gain the confidence in the FE models. Measuring the sound output and the total harmonic distortion made it to possible to confirm and increase knowledge of the damage done by shock loading. Looking at component level it was possible to measure the eigenmodes/eigenfrequency of the armature alone. The tool and experimental set-up led to good results which had a good correspondence with the finite element model. The scan of membrane surface before and after shock allowed for seeing the deformation of the membrane and couple this to the plastic deformation in the model. The receiver integrity is affected by removing the cover, however this will again help with gaining the confidence needed to thrust the predictions of the FE models.

Once the confidence in the model is good enough, the results of the simulation could be properly analysed. The internal energy is a good result when comparing different designs or situations with each other, since this will give direct insight in the energy stored due to deformation. A closer look at the von Mises stress and plastic strain is necessary to identify the critical regions. The use of non-linear material properties such as plasticity models allows to investigate the plastic strain, thus permanent deformation after shock. The Balanced armature receiver, as expected, shows high stresses and strains in the locations where it deforms most. This would be the hinges of the armature and membrane.

With the methodology to create the FE models plus the gained knowledge about the critical regions it is possible to make fast adaptations in virtual prototyping. Adding protection to the armature can now be modelled with relative ease. As found in the simulations the shock plates do reduce the damage of the response of the armature significantly. The shock plates addition restrict the movement the armature can make. Changing the material of these shock plates might even benefit the damping of the movement of the armature even further. The changes of the membrane also show increasing and decreasing robustness. If robustness is desired a thicker membrane with an embossment will provide this. However, since every design choice is a trade-off, it should be realised that the consequences on the sound performance are influenced by this. Using COMSOL multiphysics modelling, prediction of these consequences can be made to help with the design choice. The fully coupled models in COMSOL are a good prediction on how altering the membrane results in the FRF of the sound pressure output.

6.2. Future Work and Recommendations

Changing the stiffness of the membrane can increase the robustness of the balanced armature receiver. However, as the performance of the receiver is dependent on the stiffness of the membrane it is advised to not simply apply one of the designs in a prototype. Advised is to create a fully coupled reference model in COMSOL. This model can be made to match certain measurements. Implementing these virtual prototypes will give a prediction of what will happen with the performance. Furthermore there is room for improving the robustness by looking into material properties of the shock plates. An advantage of the shock plates is that they barely influence the performance of the receiver as long as they do not restrict the movement of the armature too much.

One of the major challenges with testing the balanced armature receiver for failure mechanisms is the fact that it is completely closed like a black box. For future work it is possible to make a 3D CT scan. From the CT-images a 3D computer model can be generated. The balanced armature receiver can than be shocked and scanned again. The main advantage is that it is now possible to visualise and measure the inside of the receiver without opening, and thus likely deforming, the receiver. The downside is that this method is expensive and not very time efficient.

For the modelling and simulation part in the future it is advised to further investigate the foil on top of the membrane. The foil is the very thin polyurethane component of the receiver that covers the membrane. Since there were too many unknowns about the material behaviour and implementation in the FE models the foil has been left out in this study. It is recommended to investigate implementation of this in the FE models for drop and shock. One of the possibilities might be to use shell elements for this. It is also advised to investigate the material properties of the drive pin. The material data used for the drive pin, CuSn6 has only linear material properties for now. The results show high stresses in the drive pin as well, so further investigation to find the behaviour of the CuSn6 material after yielding is advised.

Bibliography

[1] Dr. Drian van der Woude, Drs. Thijs Stoop, and Dr. Jan-Peter Heida. De maatschappelijke impact van leeftijdsgerelateerde slechthorendheid in nederland. Technical report, SiRM, 07 2019.

[2] A. Vonlanthen. *Hearing intrument technology.* Singular publishing group, June 1996. ISBN 3-274-00089-2.

[3] Jont Allen and Noori Kim. Historic transducers: Balanced armature receiver (bar). *The Journal of the Acoustical Society of America*, 136:2251–2251, 10 2014. doi: 10.1121/1.4900126.

[4] Sonion. Sonion balanced armature receiver poster, sonion academy poster. *Sonion.com*, August 2013. doi: https://www.sonion.com.

[5] Joe Jensen. *Nonlinear Distortion Mechanisms and Efficiency of Balanced-Armature Loudspeakers.* Technical University of Denmark, Department of Electrical Engineeringr, 2014. ISBN 978-87-92465-48-1.

[6] Mike Ashby, Hugh Shercliff, and David Cebon. *Materials Engineering, Science, Processing and Design.* Elsevier, fourth edition, 2014. ISBN 978-0-08-097773-7.

[7] N. Muthuram and S. Saravanan. Free fall drop impact analysis of board level electronic packages. *Microelectronics Journal*, 129, November 2022. doi: https://doi.org/10.1016/j.mejo.2022.105601.

[8] Oguzhan Mulkoglu, Mehmet A. Guler, and Hasan Demirbag. Drop test simulation and verification of a dishwasher mechanical structure. *10th European LS-DYNA Conference 2015, Würzburg, Germany*, June 2015. doi: NotAvailable,Âľ2015CopyrightbyDYNAmoreGmbH.

[9] Seungbae Park, Chirag Shah, Jae Kwak, Changsoo Jang, and James Pitarresi. Transient dynamic simulation and full-field test validation for a slim-pcb of mobile phone under drop / impact. *Proceedings - Electronic Components and Technology Conference*, July 2007. doi: 10.1109/ECTC.2007.373907.

[10] Aishwarya Gosavi, Atul Kulkarni, Yogiraj Dama, Abhijeet Deshpande, and Bhagwan Jogi. Comparative analysis of drop impact resistance for different polymer based materials used for hearing aid casing. *Materials Today: Proceedings*, October 2021. doi: https://doi.org/10.1016/j.matpr.2021.09.519.

[11] J. Luo, D.W. Shu, B.J. Shi, Q.Y Ng, R.Zambri, and J.H.T Lau. Study of the shock response of the hdd with ansys-lsdyna. *Journal of Magnetism and Magnetic Materials*, 303, February 2006. doi: https://doi.org/10.1016/j.jmmm.2006.01.104.

[12] W. J. Plumbridge, R. J. Matela, and A. Westwater. *Non-linear Finite Element Analysis. In: Structural Integrity and Reliability in Electronics.* Springer, Dordrecht, 1st edition, 2004. ISBN 978-1-4020-2611-9.

[13] Min-Chun Pan and Po-Chun Chen. Drop simulation/experimental verification and shock resistance improvement of tft-lcd monitors. *Microelectronics Reliability*, 47, February 2007. doi: https://doi.org/10.1016/j.microrel.2006.12.003.

[14] Kamarajan Balakrishan, Arvind Sharma, and Rajib Ali. Comparison of explicit and implicit finite element methods and its effectiveness for drop test of electronic control unit. *Procedia Engineering*, 173, December 2017. doi: 10.1016/j.proeng.2016.12.042.

[15] Tong Yan Tee, Jing en Luan, Eric Pek, Chwee Teck Limb, and Zhaowei Zhong. Advanced experimental and simulation techniques for analysis of dynamic responses during drop impact. *Electronic Components and Technology Conference*, 2004. doi: 10.1109/ECTC.2004.1319475.

[16] Chang-Lin Yeh and Yi-Shoa Lai. Support excitation scheme for transient analysis of jedec board-level drop test. *Microelectronics Reliability*, 46, February - April 2006. doi: https://doi.org/10.1016/j.microrel.2004.12.021.

[17] Andres Garcia-Perez, Felix-Sorribes-Palmer, Gustavo Alonso, and Ali Ravanbakhs. Fem simulation of space instruments subjected to shock tests by mechanical impact. *International Journal of Impact Engineering*, 126, April 2019. doi: https://doi.org/10.1016/j.ijimpeng.2018.12.008.

[18] Mohammed A Gharaibeh. *Handbook of Material Failure Analysis*. Butterworth-Heinemann, 2020 edition, 2020. ISBN 9780081019375.

[19] Ahmer Syed, Seung Mo Kim, Wei Lin, Jin Young Khim, Eun Sook Song, Jae Hyeon Shin, and Tony Panczak. A methodology for drop performance prediction and application for design optimization of chip scale packages. *Proceedings Electronic Components and Technology, 2005. ECTC*, 2005, June 2005. doi: 10.1109/ECTC.2005.1441308.

[20] Benson and David J. *Explicit Finite Element Methods for Large Deformation Problems in Solid Mechanics. In Encyclopedia of Computational Mechanics Second Edition. Part 1. Solids and Structures*. John Wiley & Sons, Ltd., 2017. doi: 10.1002/9781119176817.ecm2003.

[21] K.H. Low, Aiqiang Yang, K.H. Hoon, Xinwei Zhang, Judy K.T. Lim, and K.L.Lim. Initial study on the drop-impact behavior of mini hi-fi audio products. *Advances in Engineering Software*, 32, May 2001. doi: https://doi.org/10.1016/S0965-9978(01)00024-2.

[22] K. Solanki, D.L. Oglesby, C.L. Burton, H. Fang, and Mark Horstmeyer. Crashworthiness simulations comparing pam-crash and ls-dyna. *SAE Technical Papers*, March 2004. doi: 10.4271/2001-01-1174.

[23] Jingjing Wen, Houpu Yao, Bin Wu, Ze Ji, Lihua Wen, Man Xu, Yi Jin, and Xunliang Yan. Dynamic analysis and structure optimization on trapezoidal wave generator for eliminating the over deviation of the residual wave in shock test measurement. *Measurement*, 182:109665, 2021. ISSN 0263-2241. doi: 10.1016/j.measurement.2021.109665.

[24] INC Ansys. Ansys explicit dynamics analysis guide. *Ansys, INC*, January 2023. doi: Ansys,INC.

[25] Da Yu, Jae B. Kwak, Seungbae, and John Lee. Dynamic responses of pcb under product-level free drop impact. *Microelectronics Reliability*, March 2010. doi: 10.1016/j.microrel.2010.03.003.

[26] Andrzej Grzadziela and Marcin Kluczyk. Shock absorbers damping characteristics by lightweight drop hammer test for naval machines. *Materials*, February 2021. doi: https://doi.org/10.3390/ma14040772.

[27] Christian Lalanne. *Mechincal Shock*, volume 2. ISTE Ltd and John Wiley & Sons, Inc., 2009. ISBN 978-1-84821-123-0.

[28] Tae-Ho Yang, Young-Shin Lee, Kon-Whi Yeon, Hyun-Myung Kim, Jun-Yeop Kim, and Hyuk-Beom Kwon. Estimation of the saw-tooth shock wave using a lead shock programmer. *Journal of Mechanical Science and Technology*, 30, January 2016. doi: 10.1007/s12206-016-0420-2.

[29] JEDEC Standard JESD22-B111. Board level drop test method of components for handeld electronic products. *JEDEC*, 2003. doi: JEDECSolidStateTechnologyAssoc.

[30] Yong Liu, Qiuxiao Qian, Jihwan Kim, and Stephen Martin. Board level drop impact simulation and test for development of wafer level chip scale package. *Electronic Components and Technology Conference*, January 2010. doi: 10.1109/ECTC.2010.5490852.

[31] Dong-Wei Shu, Bao-Jun Shi, Hui Meng, Da-Zhi Jiang Fook Fah Yap, Quock Ng, Razman Zambri, Joseph H.T. Lau, and Chao-Shan Cheng. Shock analysis of a head actuator assembly subjected to half-sine acceleration pulses. *International Journal of Impact Engineering*, 34, February 2007. doi: https://doi.org/10.1016/j.ijimpeng.2005.07.009.

[32] E. Tempelman, M.M.S. Dwaikat, and C. Spitas. Experimental and analytical study of free-fall drop impact testing of portable products. *Experimental Mechanics*, 52, January 2012. doi: 10.1007/s11340-011-9584-y.

[33] R.C. Hibbeler and Kai Beng Yap. *Mechanics for Engineers; Dynamics*. Pearson Education, 2012. ISBN 978-981-06-9261-2.

[34] Ph.D. Jeremy Agnew. The causes and effects of distortion and internal noise in hearing aids. *Trends in Amplification*, 3, September 1998. doi: 10.1177/108471389800300302.

[35] H. Dillon and J. Macrae. *Derivation of design specifications for hearing aids*, volume 102. National Acoustics Laboratory Report, 1984. ISBN 0644012927.

[36] Romain Lietchi, Stephane Durand, Thierry Hilt, Fabrice casset, Christophe Poulain, Gwenael Le Ruhn, Franklin Pavagau, Hugo Kuentz, and Mikael Colin. Total harmonic distortion of a piezoelectric mems loudspeaker in an iec 60318-4 coupler estimation using static measurements and a nonlinear state space model. *Micromachines*, 12, November 2021. doi: https://doi.org/10.3390/mi12121437.

[37] Zoe Yee Ting Chan and Bradley McPherson. Over-the-counter hearing aids: A lost decade for change. *BioMed research international*, 2015, January 2015. doi: https://doi.org/10.1155/2015/827463.

[38] Andres Garcia-Perez, Felix-Sorribes-Palmer, Gustavo Alonso, and Ali Ravanbakhs. Overview and application of fem methods for shock analysis in space instruments. *Aerospace Science and Technology*, 80, September 2018. doi: https://doi.org/10.1016/j.ast.2018.07.035.

[39] C.Y.Zhou, T.X.Yu, and Ricky S.W. Lee. Drop/impact tests and analysis of typical portable electronic devices. *International Journal of Mechanical Sciences*, 50, February 2007. doi: 10.1016/j.ijmecsci.2007.09.012.

A

Explanation of the Numerical Solvers

A.1. Explicit solvers in FEM

When solving time dependent ordinary or partial differential equations in numerical analysis, one can choose to use an explicit approach or an implicit. When looking at transient analysis it is important to understand that dynamics is split into time steps [21]. With explicit integration the solution advances in time at t^n to t^{n+1}. Ansys LS-Dyna mostly uses the Central Difference Method to integrate over time.

The Central Difference Method

The central difference time integration scheme is used by the ls-Dyna explicit solver. Also known as the leapfrog method. The scheme is described by the explicit solver guide as follows [24]:

A.2. Difference between Explicit and Implicit Solvers in FEM

A simple 1 DOF will be used as an example to illustrate the difference.

- Implicit Time Integration

$$y(t_{n+1}) = y(t_n) + \Delta t * y'(t_{n+1}) \tag{A.1}$$

- Explicit Time Integration

$$y(t_{n+1}) = y(t_n) + \Delta t * y'(t_n) \tag{A.2}$$

Example: Find $y(t = 1)$

$$y' = sin(y), t = 0, y_0 = 1$$
$$y_1 = y_0 + \Delta t * y'$$

Implicit (needs to be solved):

$$\begin{aligned} y_1 &= y_0 + \Delta t * y_1' \\ &= y_0 + \Delta t * sin(y_1) \\ y_1 &= 1 + 1 * sin(y_1) \end{aligned}$$

Explicit (Directly obtained):

$$\begin{aligned} y_1 &= y_0 + \Delta t * y_0' \\ &= y_0 + \Delta t * sin(y_0) \\ y_1 &= 1 + 1 * sin(1) \\ y_1 &= 1.84 \end{aligned}$$

A.2.1. Implicit time integration solvers

In contrast to explicit algorithms, implicit algorithms require matrix manipulation, factorisation of the stiffness matrix and iteration. Implicit solvers create large matrices of all the equations and thus degrees of freedom, which must converge in order to be solved correctly. This can make them more computationally expensive than explicit solvers. An advantage of using the implicit solver instead of an explicit solver, is that it is not dependent on the smallest element. Independence of the element size allows the solver to permit larger time steps.

The paper of Kamarajan *et al.* shows that implicit and explicit methods are capable of solving this problem. However there is not one best way to solve every problem, so trade-offs and a deep understanding of your problem are required to make the best decision. Within the different methods it is necessary to understand the problem that you are trying to solve.

Implicit FEM Software	**Literature**
Abaqus	Kim Low *et al.* [21]
ANSYS	Seungbae Park *et al.*[9]
COMSOL	Aishwarya Gosavi *et al.* [10]
NASTRAN Code	Andres Garcia *et al.* [17] [38]

Table A.1: Overview Implicit Solvers

B
Material models

Material Models

	Density [kg/m^3]	Young's modulus [Pa]	Poisson's ratio	Bulk Modulus [Pa]	Shear Modulus [Pa]
NiFe49 - High Permeability 49	8.20E+03	1.41E+11	3.00E-01	1.17E+11	5.42E+10
NiFe80 - Hymu Annealled	8.40E+03	1.62E+11	3.00E-01	1.35E+11	6.23E+10
Permanen Magnet Alnico 8 (cast) - G	7.10E+03	1.73E+11	2.96E-01	1.41E+11	6.68E+10
CuSn6	8.80E+03	1.15E+11	3.00E-01	9.58E+10	4.42E+10
Vectra E130i – LCP-GF30	1.15E+03	2.00E+09	4.00E-01	3.33E+09	7.14E+08
Coil (Copper wires in Sonion)	4.10E+03	1.10E+11	3.50E-01	1.22E+11	4.07E+10
Nickel, pure, grade 200, hard - G	8.90E+03	2.05E+11	3.10E-01	1.79E+11	7.81E+10
VHB 3M - Tape	8.00E+02	6.02E+08	4.90E-01	1.00E+10	2.02E+08

NiFe49 - High Permeability 49

Multilinear Isotropic Hardening	Plastic Strain [m/m]	Stress [Pa]	Stress [Mpa]
	0	253180205.4	253.18021
	0.0008	256300000	256.3
	0.002319561	257021240.9	257.02124
	0.003382039	263162614	263.16261
	0.012548733	292919632.4	292.91963
	0.033262587	359108871.8	359.10887
	0.084668473	485803982.9	485.80398
	0.138477257	583282649	583.28265
	0.192373243	654265407.1	654.26541
	0.273323537	725462240	725.46224

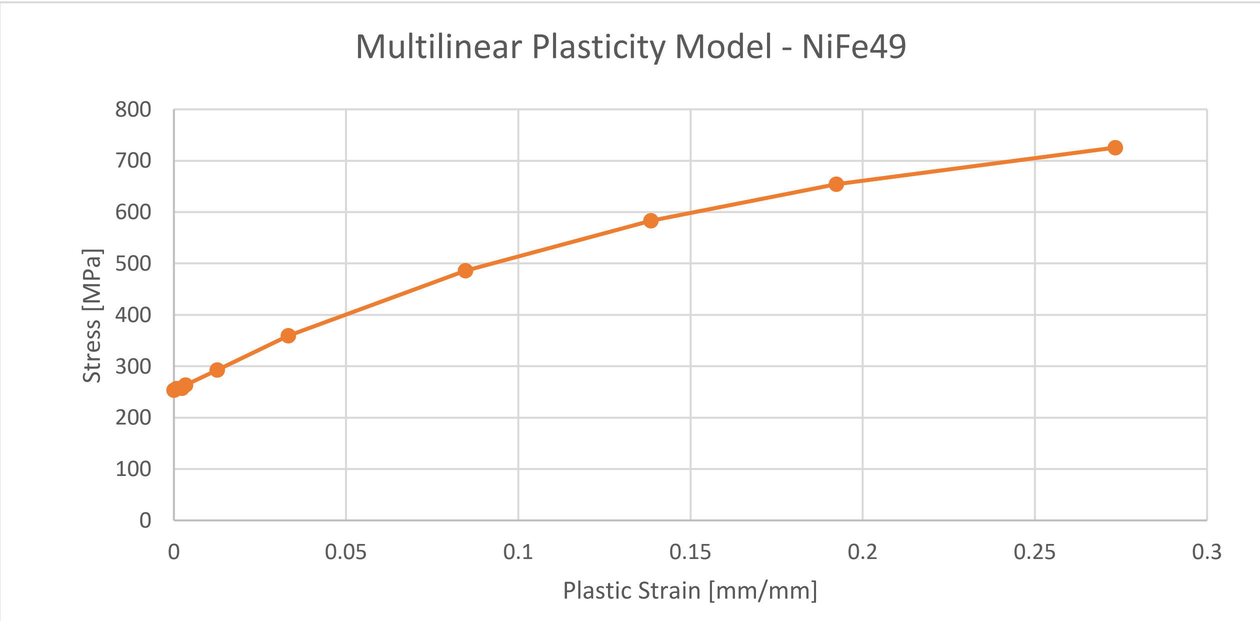

Material Models

NiFe80 - Hymu Annealled

Plastic Strain [m/m]	Stress [Pa]	Stress [Mpa]
0	258900000	258.9
0.001	293900000	293.9
0.00266	307000000	307
0.01091	354300000	354.3
0.03658	437400000	437.4
0.06541	515900000	515.9
0.10741	618700000	618.7
0.16147	729000000	729
0.20963	806100000	806.1
0.29792	892200000	892.2

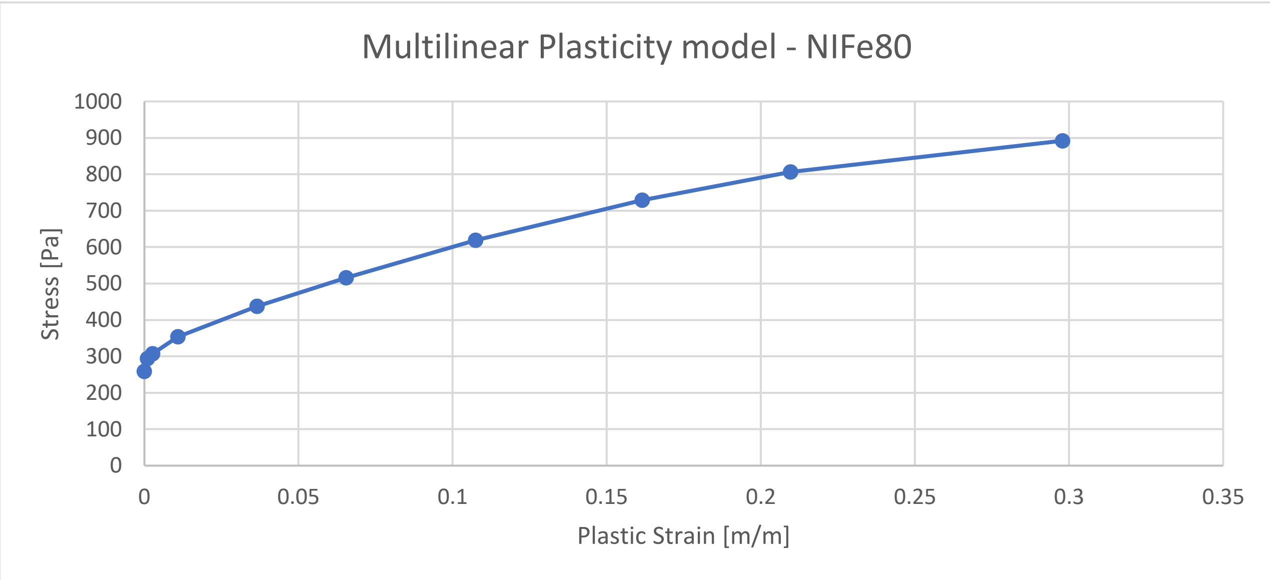

Nickel, pure, grade 200, hard

Plastic Strain [m/m]	Stress [Pa]	Stress [Gpa]
0	0	0
0.003	617700000	0.6177
0.015	6.38E+08	0.63774

Tangent modulus 1.67E+09

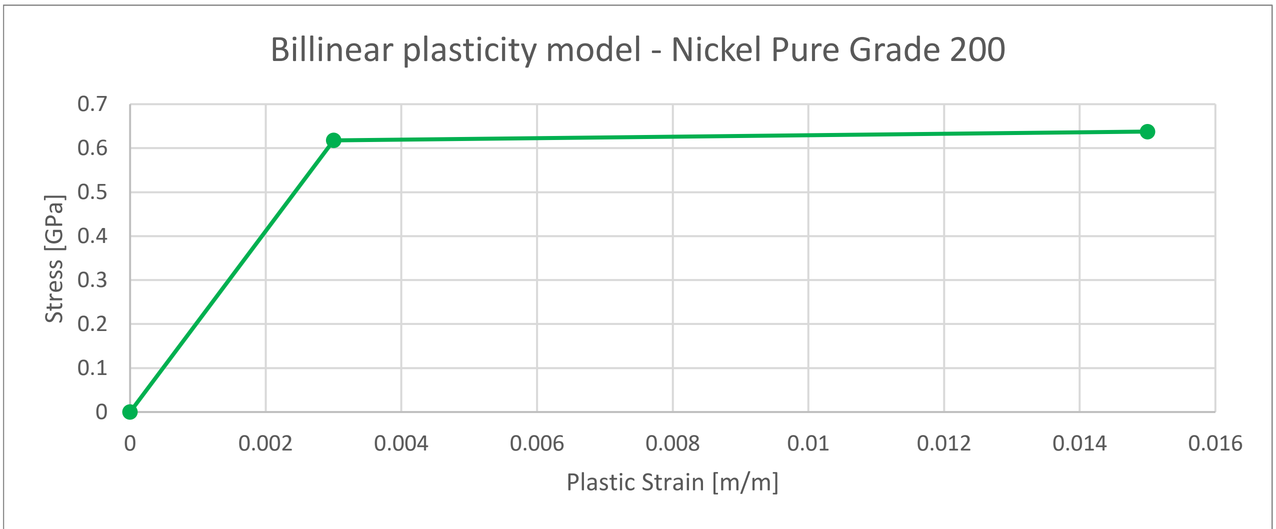

C

Post-Processing

C.1. Post-processing

Different types of energy can be checked to see if the model is running properly. Hourglass energy is already explained in 3.2.3. Different type of energy to check is of course the Total Energy. The energy ratio is probably the fastest way to check if the model is wrong. The ratio should always be as close as possible to the value of 1. The sliding energy to see if the contacts are defined properly. This energy should always be positive and should end without a rise. This check is done for all the model but the following example is between the reference model and a model with shock plates.

Energy Check

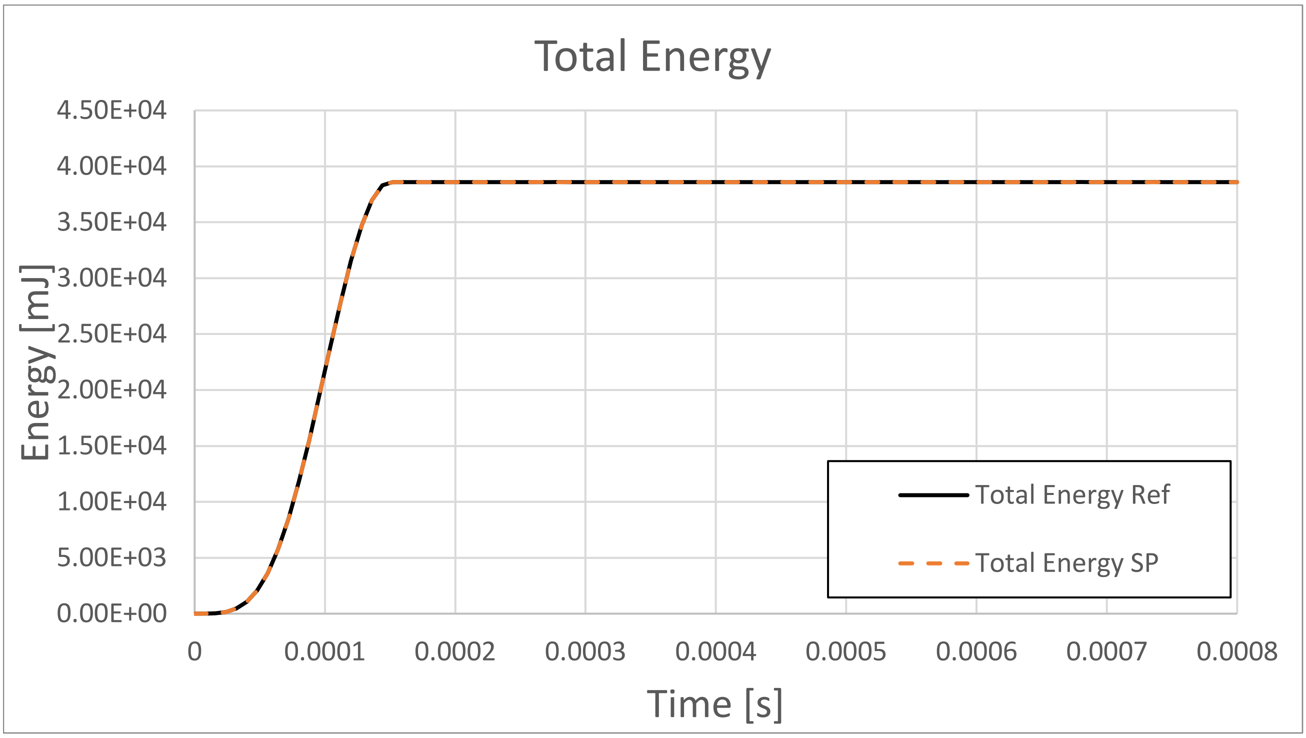

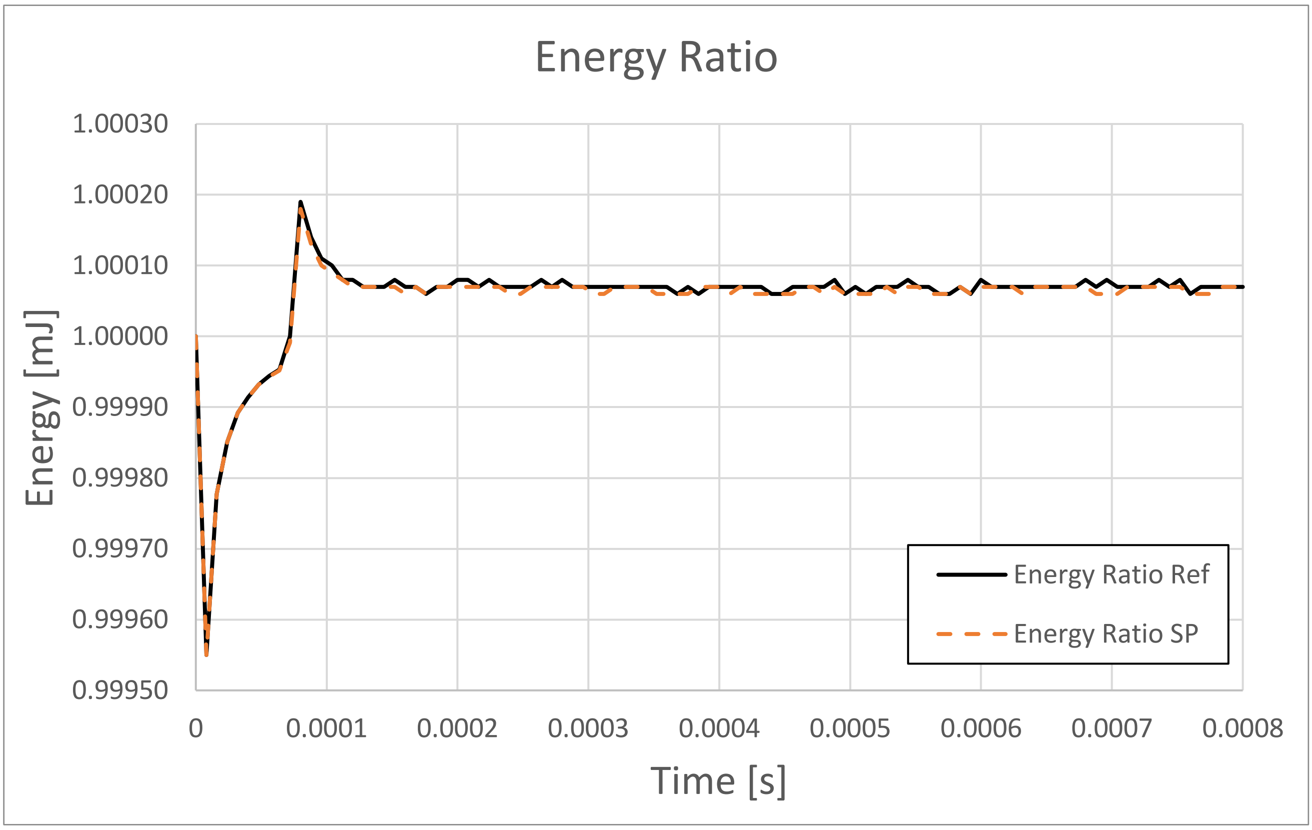

Energy Check

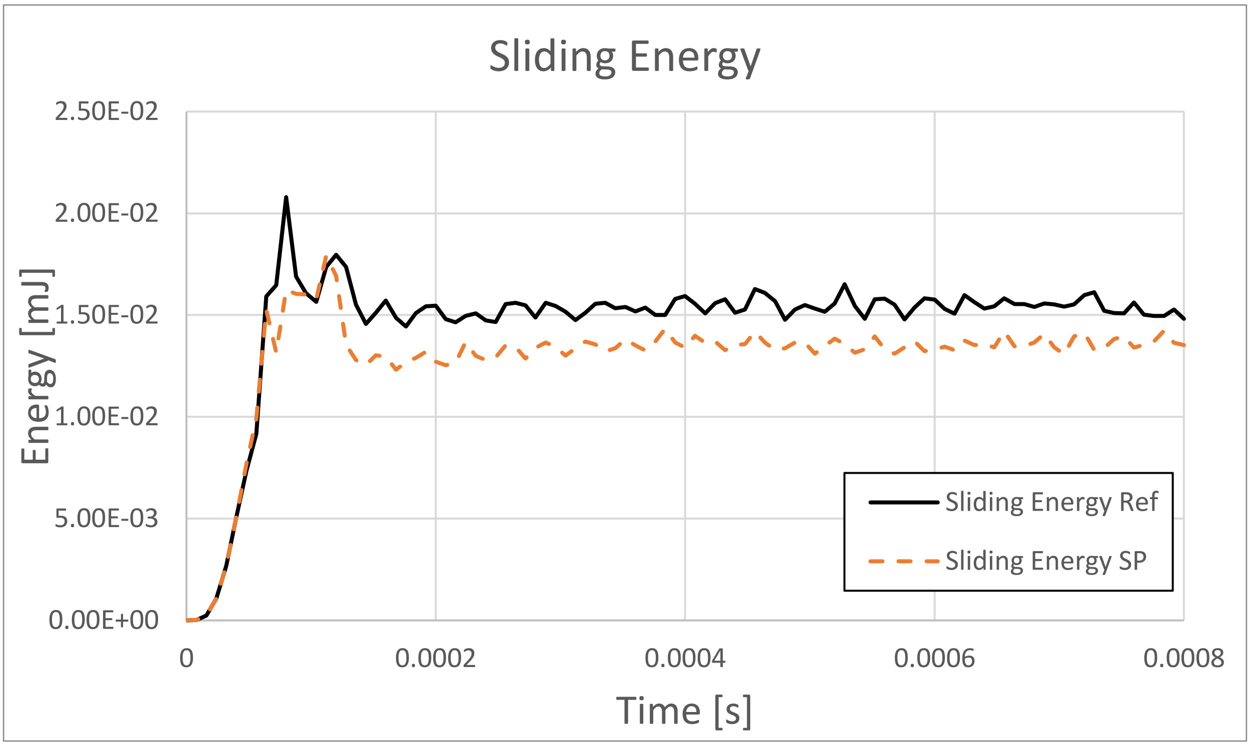

Energy Check

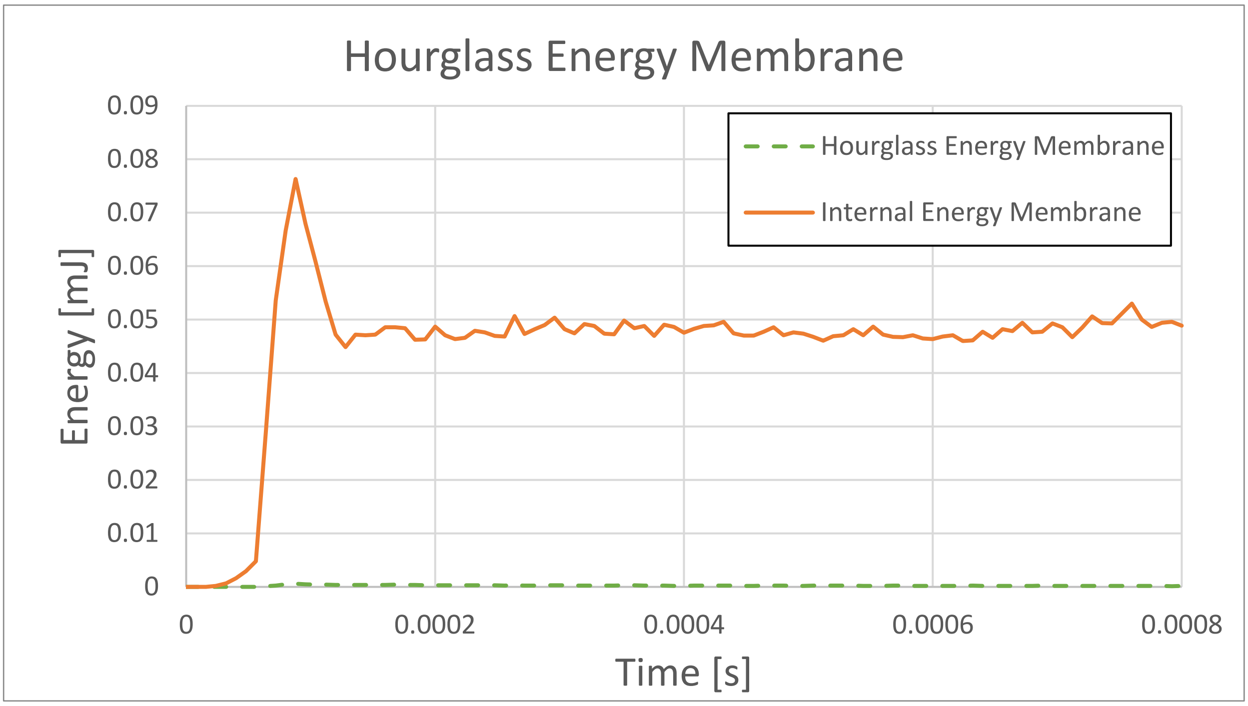

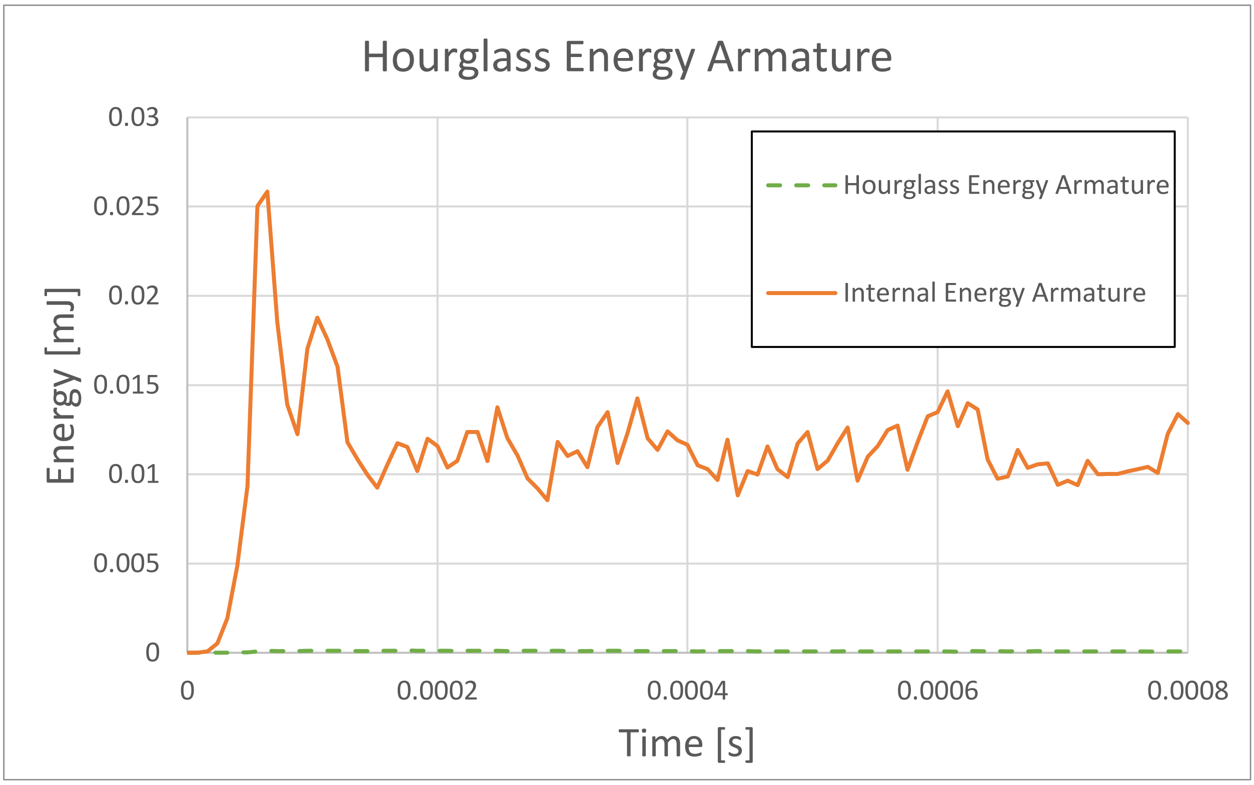

D
Shock pulses

D.1. Alternative Shock pulses

The Haversine

The haversine pulse waveform is a shock pulse where the curve is similar to a sinus wave. The initial starting position of the pulse is the minimum of a sine wave up until the next minimum. The haversine function therefor has a smoother rise and smoother decent then the half sine function. It must be mentioned that this type of pulse is less common within this field of research. To better approach this waveform, the material properties of the colliding objects must have viscoelastic properties (such as rubbers). This is necessary to create the smoother rise and decent.

$$\left.\begin{array}{ll} \ddot{x}(t) = \frac{\ddot{x_m}(t)}{2}\left(1 - cos\frac{2\pi}{\tau}t\right) & for \quad 0 < t < \tau \\ \ddot{x}(t) = 0 & elsewhere \end{array}\right\} \tag{D.1}$$

The saw-tooth

The (terminal Peak) saw-tooth shock wave is a ramp input with a sharp decrease. Yang *et el.* presents a study on the possibility of using a lead shock programmer with conical and truncated conical shape [28]. In his study the material is kept as a constant, the comparison is between the different lead shock programmer geometrical dimensions. The paper present a proper example of the influence of geometry. The idealised equation used for this pulse is as follows:

$$\left.\begin{array}{ll} \ddot{x}(t) = \ddot{x_m}(t)\frac{t}{\tau} & for \quad 0 < t < \tau \\ \ddot{x}(t) = 0 & elsewhere \end{array}\right\} \tag{D.2}$$

The trapezoidal

The trapezoidal waveform is frequently described among acceleration-time pulses. The trapezoidal waveform has a linear rising, a constant and a linear decreasing acceleration over the time of the pulse. Jingjing *et al.* argues that this waveform can produce a higher response over a wider spectrum[23]. The shape of the pulse can be altered by geometry and material choices of the programmer. To realise the trapezoidal waveform it requires a proper engineered programmer. This design will cost in many cases significant amount of time- and resources. The programmer is often referred to as Trapezoidal Waveform Generator (TWG). In order for their TWG to achieve the desired waveform, a piston is designed. When designing a piston it creates an increase in complexity and non-linearities. For example non-linear materials such as rubber, the gas chamber and the damping of residual waves must be taken into account. Jingjing *et al.* show in their paper a design and validation of their Trapezoidal Wave Generator, that indeed is able to handle the three types of acceleration and the residual waves. It can be concluded that type of pulse for shock loading is relevant for the type of desired experiment.

Known test set-ups

Different techniques and methods are used to approximate a desired acceleration pulse waveform. Drop tables are a widely used and standardised with shock tests on electronics, for example JEDEC [29]. The paper of chang-Lin Yeh *et al.* has a proper visualisation of the test set-up [16]. The test object if mounted to the drop table, base plate. The drop table is guided by guide rods, to create consistency between the drops. The strike surface is often called the programmer [27]. The programmer can be engineered to created a desired waveform such as trapezoidal [23]. The rigid base must be heavy to enough to handle the impact from the drop table.

A pendulum (see fig 4.3)can be used to apply the same principle as the drop table. The peak value can be set before hand. Because of the geometry of the end of the pendulum the rotational velocity is converted to a shock wave. Zhou *et al.* guides the object with a pendulum with this technique. [39]

When measuring the pendulum machine the unfiltered data will have the eigenfrequencies of the accelerometer in the results. This can be filtered by the oscciloscope.

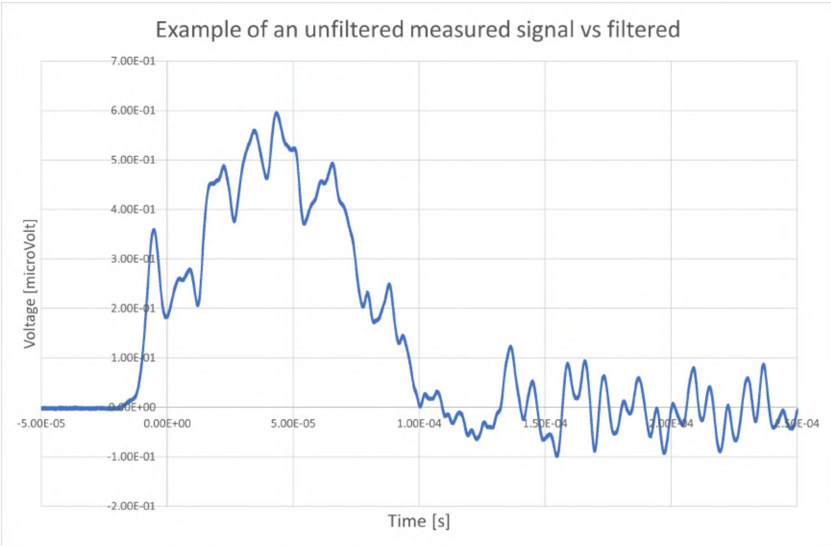

Figure D.1: Example of an unfiltered signal